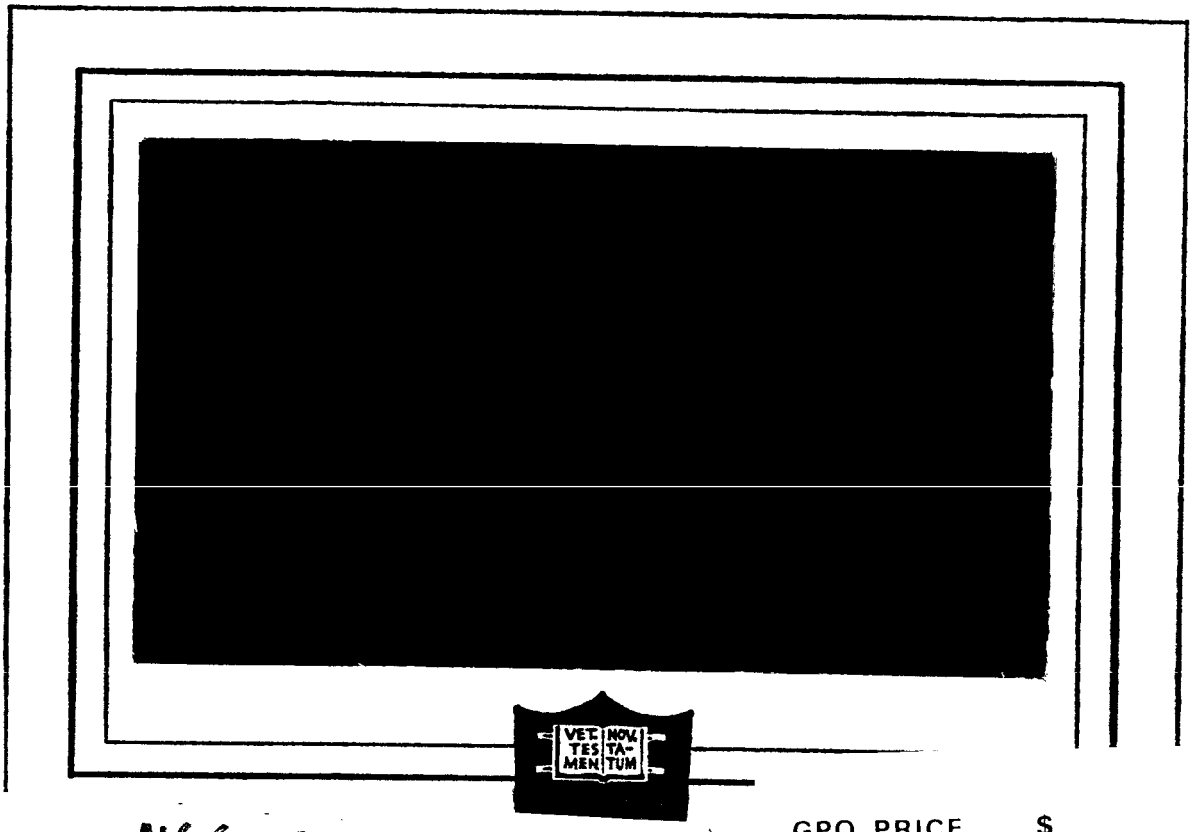

NASA CR 71097

PRINCETON UNIVERSITY

DEPARTMENT OF AEROSPACE AND MECHANICAL SCIENCES

NATIONAL AERONAUTICS
AND SPACE ADMINISTRATION

Research Grant NsG-306-63

PULSED ELECTROMAGNETIC GAS ACCELERATION

Seventh Semi-Annual Progress Report

1 July 1965 to 31 December 1965

Report No. 634f

Prepared by: Robert G. Jahn
Robert G. Jahn
Associate Professor
and Research Leader

and: Woldemar v. Jaskowsky
Woldemar F. von Jaskowsky
Research Engineer

January 1, 1966

Guggenheim Laboratories for the Aerospace Propulsion Sciences
Department of Aerospace and Mechanical Sciences
PRINCETON UNIVERSITY
Princeton, New Jersey

Abstract 19538

A selection of physical processes implicit in pulsed plasma propulsion are under study by a variety of experimental and theoretical techniques. Some processes are studied in well-defined, closed-chamber discharges where they are highly reproducible and accessible to precise probing and analysis; others are studied in an exhaust-to-vacuum environment more closely simulating space operation. As examples, detailed measurements of radial and axial electric field components within closed-chamber discharge current sheets are combined with earlier data on magnetic field and current density distributions in the same sheets to yield a more complete picture of the gas acceleration and current conduction processes on a microscopic scale. Likewise, an ultra-high speed piezoelectric pressure transducer has been developed to establish the position of the gasdynamic pressure front with respect to the current sheet; and a 4 mm. microwave probe provides a similar correlation for the profiles of free electron density. Magnetic probe studies in one particular type of closed chamber discharge have revealed a spontaneous bifurcation of the current sheet at a critical radial position, yielding a "fast" and "slow" component of unexplained origin.

The exhaust of pulsed plasmas to a vacuum has been studied photographically and with magnetic probes and ion collectors. A tendency to stabilization of the current patterns in the exhaust plume has been observed while the plasma ejection process continues unabated. This conversion from a current sheet "sweeping" mode which initiates the acceleration process, to a steady-flow, magnetogasdynamic "pumping" mode, suggests some relevance to the currently popular "Magnetoplasmadynamic Arc."

In addition to the development of suitable diagnostic devices, effort has been expended on design and construction of certain peculiar operational equipment required for this program. A series of versatile, high performance capacitors suitable for low impedance pulse-forming lines are being developed in cooperation with an industrial laboratory. Likewise, a large Plexiglas vacuum tank has been built and installed to provide an optimum environment for the plasma exhaust studies.

Author

Students Associated With This Program

N. Black	(Graduate Assistant)
R. Burton	(Graduate Fellow)
C. Carrelli	(Visiting Scholar)
K. Clark	(Graduate Fellow)
K. Cooke	(Graduate Fellow)
A. Eckbreth	(Graduate Fellow)
W. Ellis	(Graduate Assistant)
E. Holzhauer	(Visiting Scholar)
G. Rowell	(Graduate Fellow)
P. Turchi	(University Scholar)

TABLE OF CONTENTS

LIST OF ILLUSTRATIONS

LIST OF ILLUSTRATIONS-contd.

I. INTRODUCTION

This research program has attained a level of operation and organization of its studies that precludes detailed review of all accomplishments of a given reporting period in a single document of this sort. The bulk of this information is better presented in the several journal articles, lectures and preprints for technical society meetings, and individual technical reports which have been issued during this period, and are now on file in the project office.[I-1 to I-32] This status report will therefore confine itself to presentation of a few of the most interesting activities of the past six months which serve to give the flavor of the progress of the program as a whole.

For the first time since the beginning of this program, a substantial fraction of the effort of this period has been invested in the design, construction, and testing of a facility. Heretofore, no single piece of apparatus has been required whose construction has involved any significant diversion of the usual research effort. Early in the present period, however, it became imperative to address ourselves to the implementation of a large, dielectric vacuum tank, if our program of plasma exhaust studies was to proceed to its full potential. This implementation has been a major effort of the past six months, but it is now essentially complete, and has provided us with a unique facility. It seems appropriate, therefore, to include some description of the design, construction, and testing of this facility in the final section of this report.

A second atypical activity of this reporting period was the beginning of a cooperative effort with a small capacitor manufacturing firm to design and construct more versatile, high performance energy storage units than are commercially available. In accordance with the stated proposal for this work,[I-27] several consultations with the Corson Manufacturing Corp. have led to construction of various experimental units which show promise of achieving the desired characteristics. This work is described in Section VII.

The other sections of this report deal with specific diagnostic studies, each of which consumes the major effort of one or more of the graduate students associated with this laboratory, and each of which will ultimately be the basis for a Ph.D. thesis in this area.

II. ELECTRIC FIELD PROFILES IN THE CURRENT SHEET (Burton)

Previous semi-annual reports have dealt extensively with magnetic field distributions in closed chamber pinch discharges.[I-4,12,14,29] It has been shown conclusively that a thin current sheet, carrying hundreds of kiloamperes, propagates from the outer wall to the center. The r(t) trajectory of this sheet agrees closely with that predicted by a snowplow analysis, thereby implying that heavy argon particles, ions or neutrals, are being effectively accelerated by the current sheet. The purpose of the present study is to search for internal electric fields which may contribute to, or arise from the acceleration of argon ions by the sheet.

The electric field sensor used in this experiment is essentially a coaxial double probe first developed by Lovberg.[II-1] The primary complication in the experiment is the necessity for an extremely high common mode rejection ratio to separate the desired signal from the intense background noise in the discharge. A photograph of the device as finally perfected is shown in Fig. 1 along with a conventional magnetic probe coil. Figure 2 displays a schematic of the system, indicating the essential components: 1) a ring and ball electrode pair, separated along the ring axis by 2 mm.; 2) a parallel variable resistor R, which controls the current drawn through the plasma; 3) an isolation-step down transformer to protect the oscilloscope from the plasma potential (several kilovolts); and 4) a Tektronix 555 dual beam oscilloscope, with Type L preamplifier, sweeping at 0.2 μsec/cm. The circuit subtracts the floating potentials of the two electrodes immersed in the plasma, and the resulting difference is stepped down and displayed on the scope screen as voltage versus time. This signal, divided by the electrode spacing, gives a good measurement of the electric field in the direction of the probe axis. Typical records are shown in Figs. 3 and 4, where radial or axial electric field is displayed on the upper trace, and the output of a magnetic probe coil ($\dot{B}_\theta$) is shown for comparison on the lower trace. The maximum radial electric field is 250 volts/cm. and the maximum axial electric field is 500 volts/cm.

Point by point surveys of the radial and axial electric fields have been made every 1/8" in the 5" diameter machine, in 120 μ argon, initial voltage 10 KV. The results of a radial survey midway between the electrodes are shown in Figs. 5 and 6, where radial electric field is plotted versus radius at eight selected times. In all cases the maxima of the axial and radial fields coincide. Note the axial field is not zero behind the sheet, consistent with the change in magnetic flux associated with the motion of the current pattern.

AP25-P34a-66

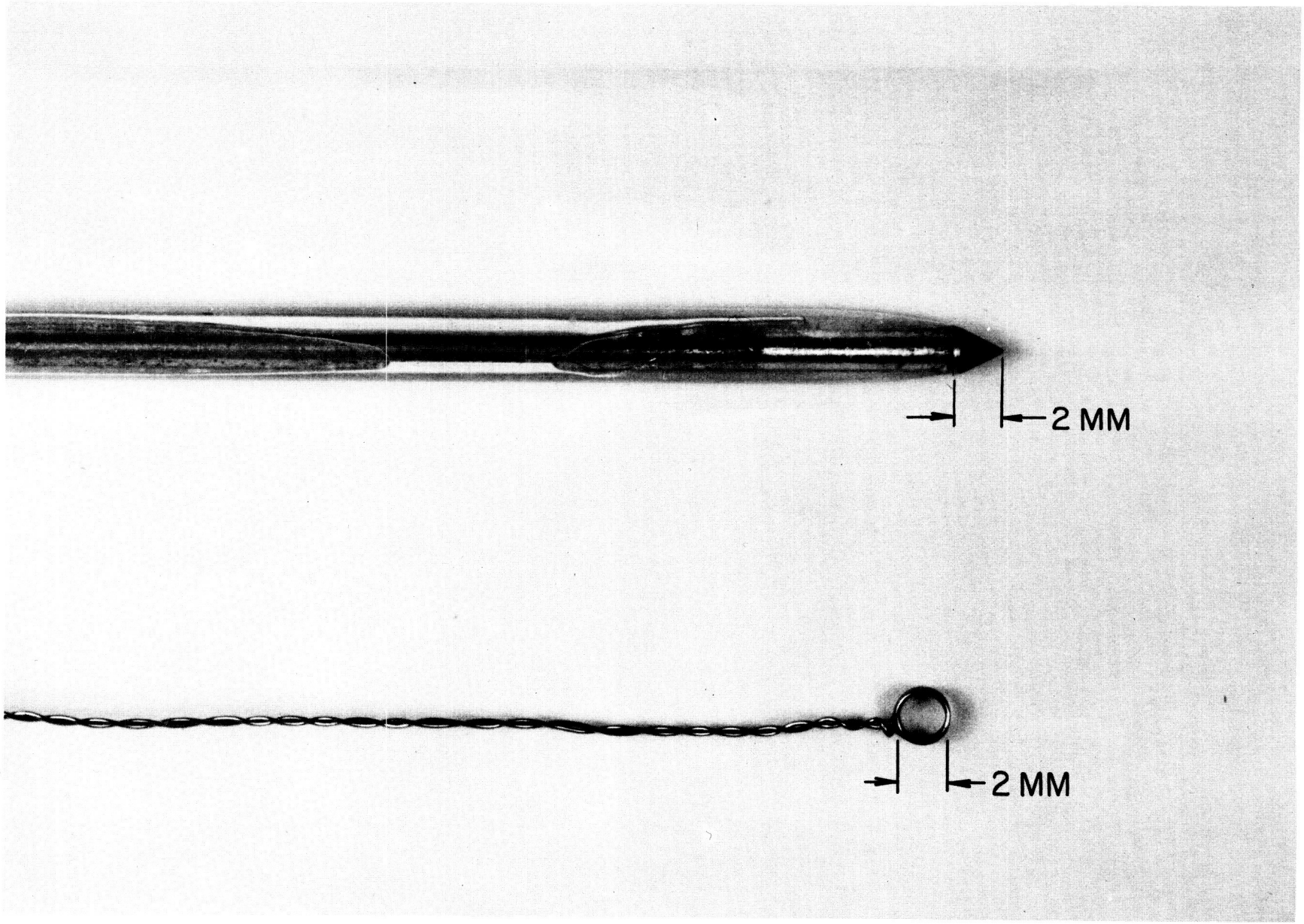

ELECTRIC FIELD PROBE AND MAGNETIC PROBE COIL

FIGURE 1

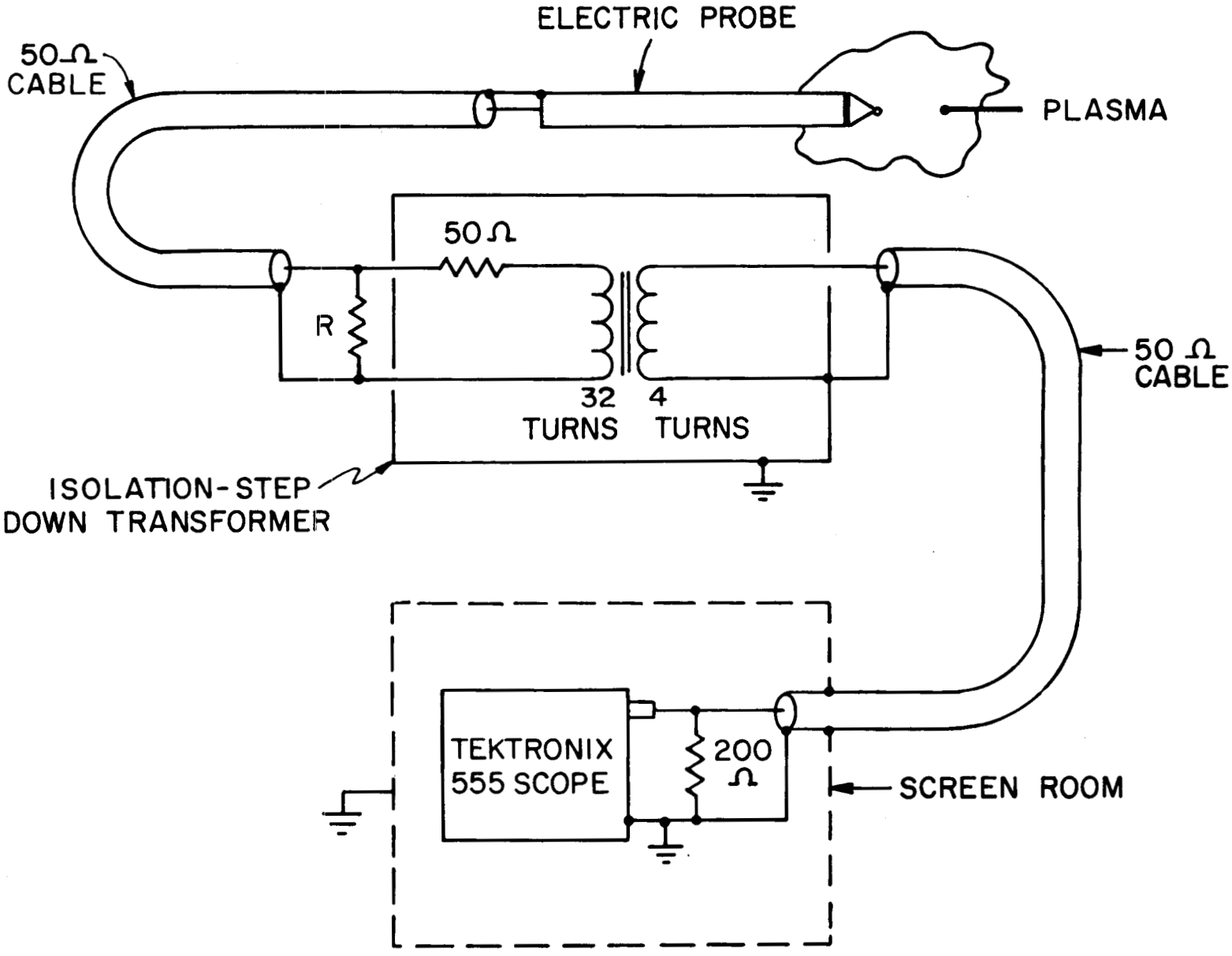

ELECTRIC PROBE CIRCUIT (SCHEMATIC)

FIGURE 2

AP25-P36-66

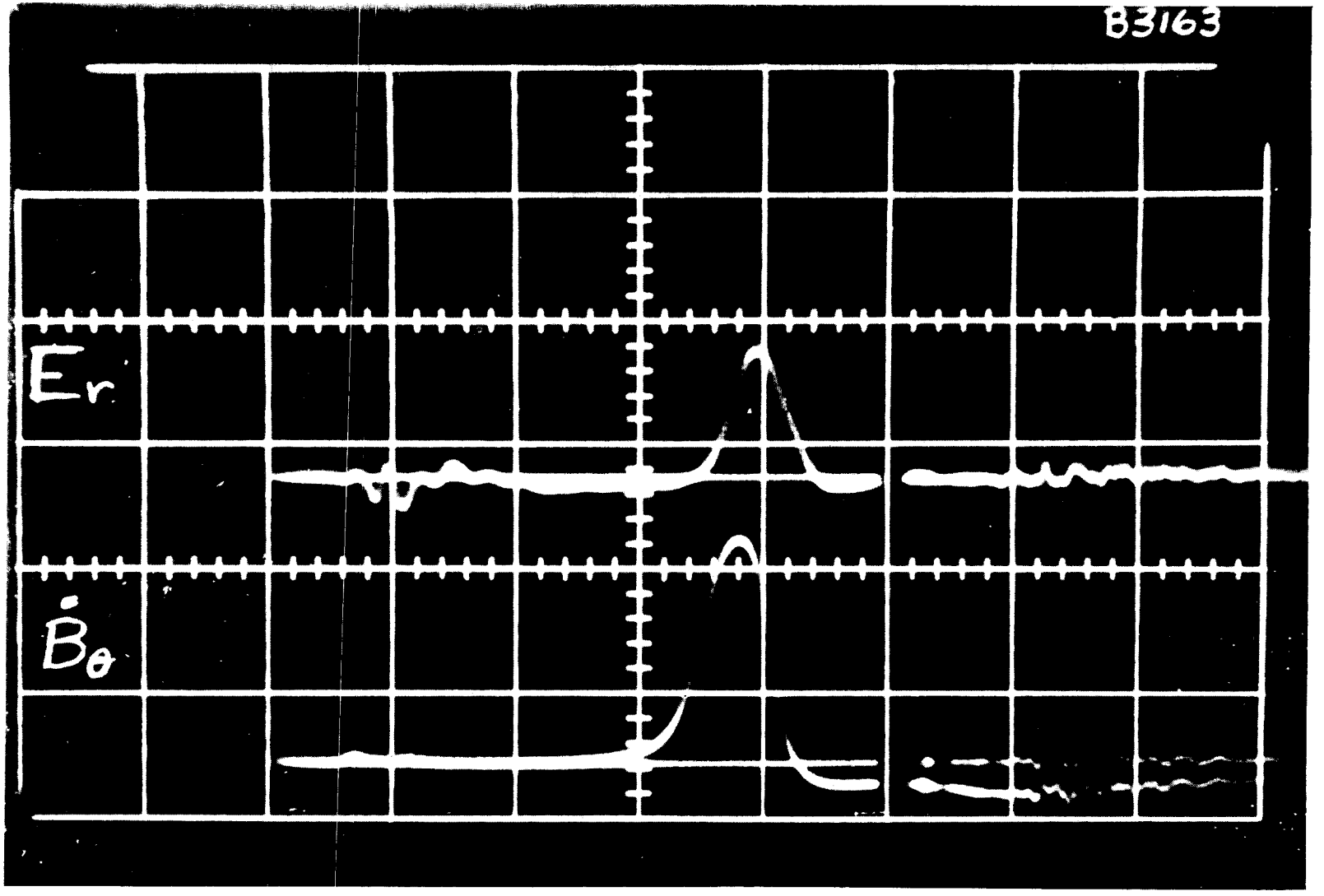

SIMULTANEOUS ELECTRIC AND MAGNETIC PROBE RESPONSES, E_r AND $\dot{B}_\theta$
120μ ARGON, 5" CHAMBER, $R/R_0 = .66$, $z/h = 0.5$

FIGURE 3

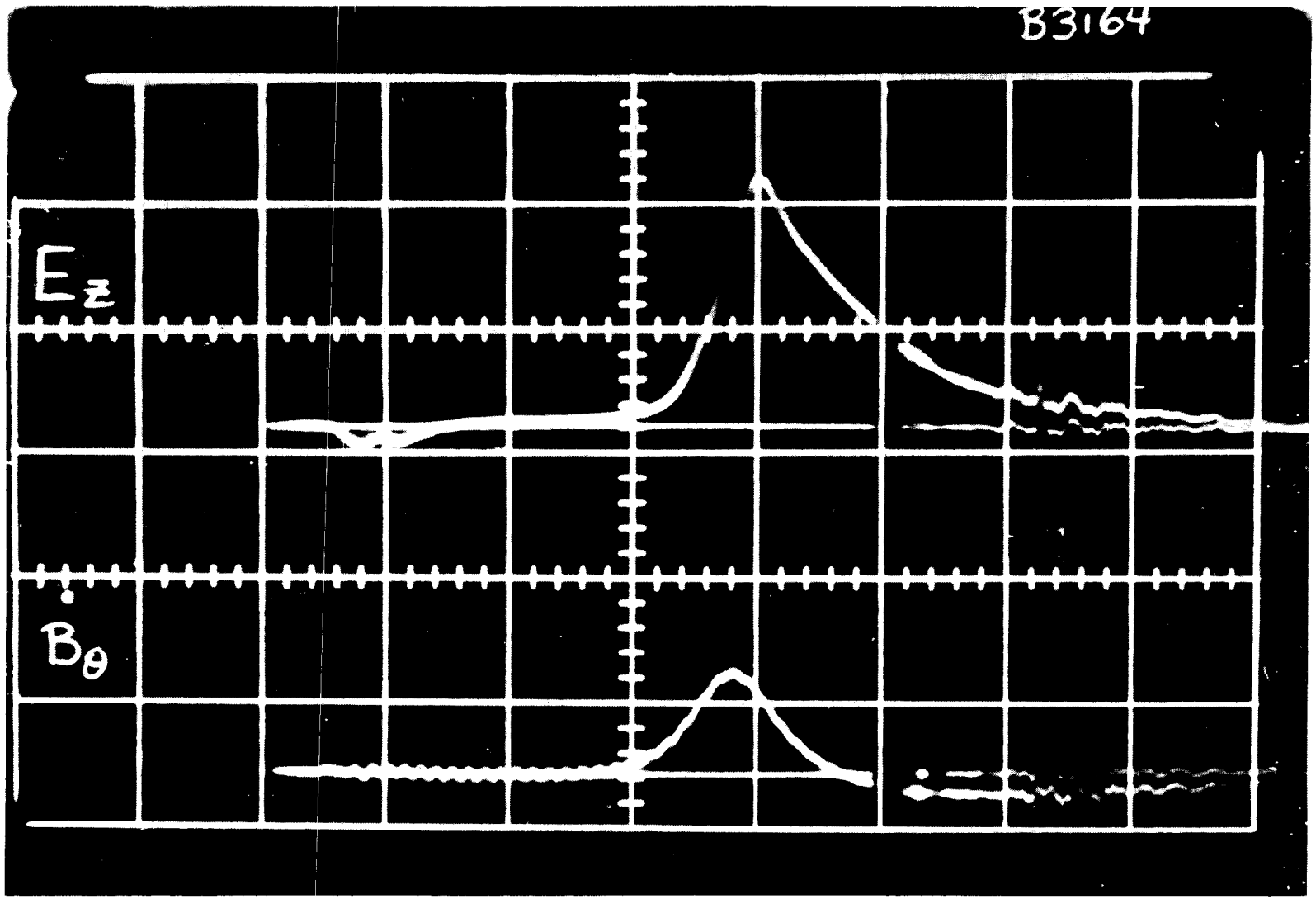

SIMULTANEOUS ELECTRIC AND MAGNETIC PROBE RESPONSES, E_z AND $\dot{B}_\theta$
120 μ ARGON, 5" CHAMBER, $R/R_0 = .66, z/h = 0.5$

FIGURE 4

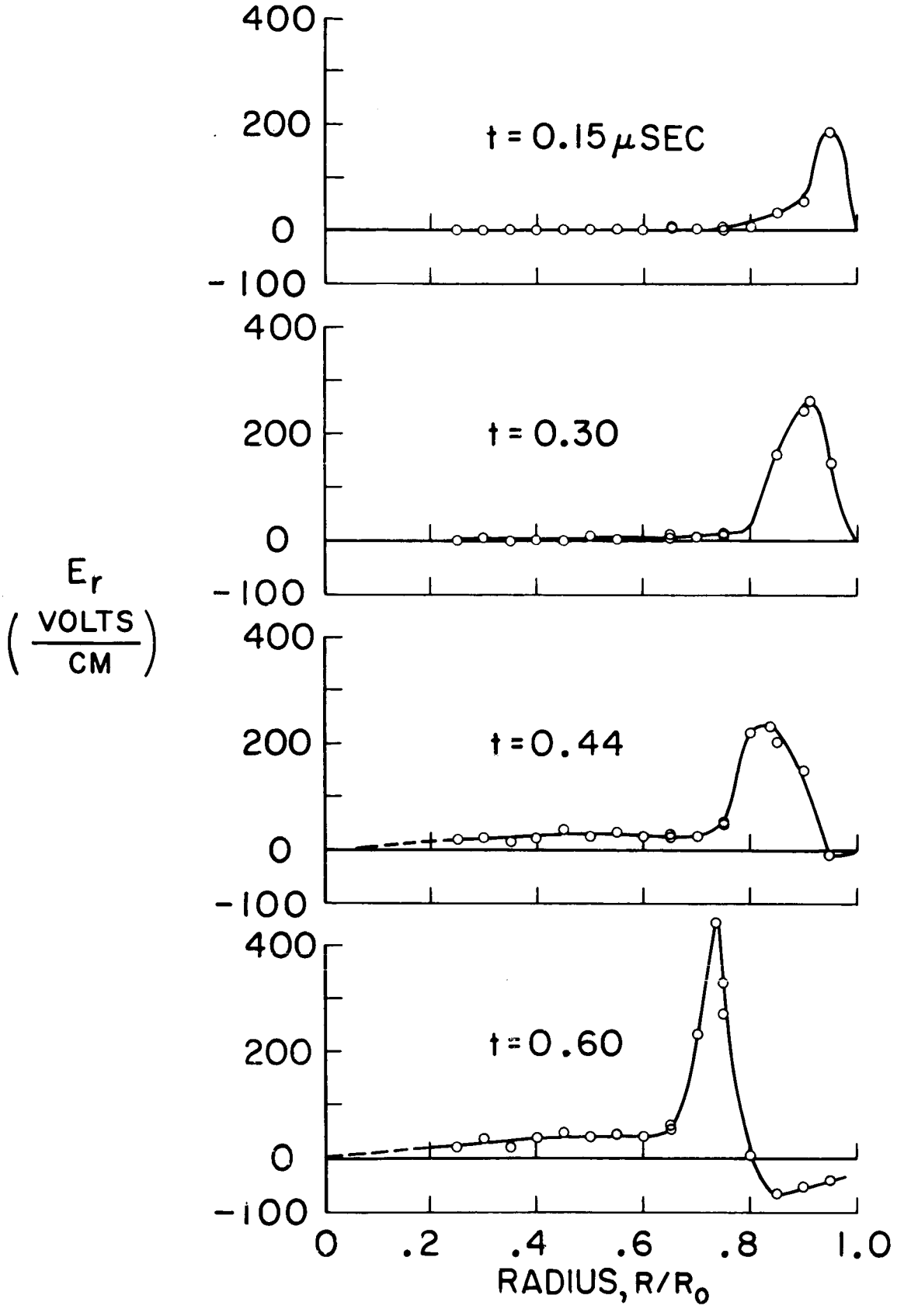

RADIAL ELECTRIC FIELD DISTRIBUTION, $z/h = 0.5$

5" CHAMBER, 120μ ARGON, 10 KV

FIGURE 5

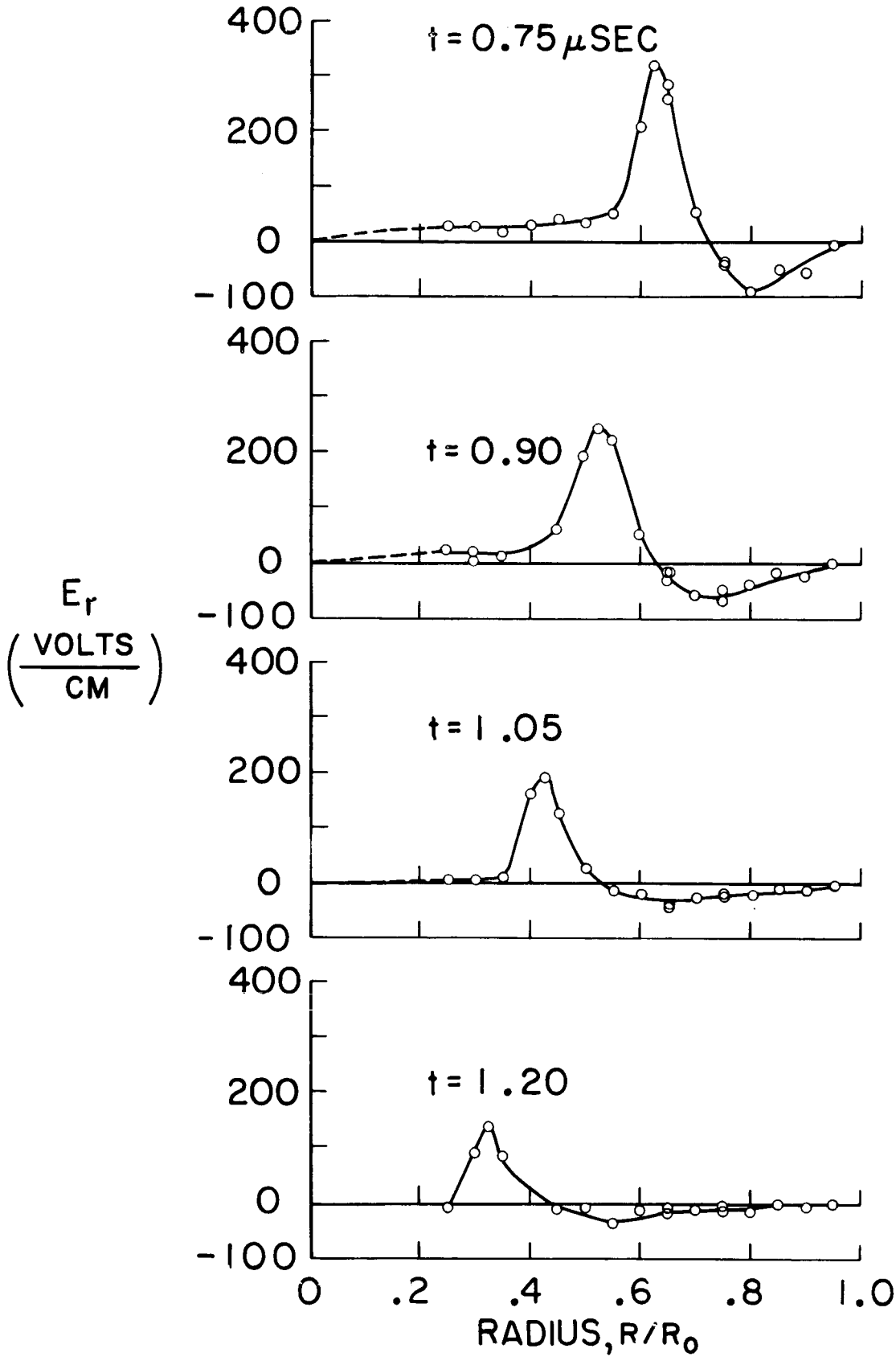

RADIAL ELECTRIC FIELD DISTRIBUTION, z/h = 0.5

5" CHAMBER, 120 μ ARGON, 10KV

FIGURE 6

Interpretation of this data is not yet complete. It is tentatively proposed that the radial electric field arises from the inertial separation of the ions and electrons as the latter are accelerated inward by the self-magnetic field. Once established, this radial electric field serves a dual purpose. First, it accelerates the entrained ions radially inward; second, it combines with the azimuthal magnetic field to constrain the electrons to an axial $\vec{E}_r \times \vec{B}_\theta$ drift, which constitutes the bulk of the arc current. The observed profiles of axial electric field seem consistent with elementary considerations of applied voltage and back emf in this environment. More detailed analysis of the origin and function of the internal electric fields will be presented in a Ph.D. thesis, to be submitted this spring. This electric probe will also see extensive use in other laboratory studies in the coming months.

III. PRESSURE MEASUREMENTS IN CLOSED CHAMBER DISCHARGES (York, Holzhauer)

The effectiveness of pulsed plasma discharges as gas accelerators clearly depends on their ability to entrain the ambient gas in the discharge chamber. Accordingly, the relation of the profiles of total gas density to those of the fields and currents is of primary interest. Unfortunately, direct determination of density profiles is inhibited by problems of the magnitude and the frequency of the sensor response in such a dynamic system. The most promising indirect determination of density is via total gas pressure. Even here, severe requirements on sensitivity, rise time, and noise discrimination of the detector are imposed by the experimental conditions, and only highly sophisticated piezoelectric techniques will suffice.

In principle there are two possibilities for the location of the sensor element, either direct contact of the transducer with the plasma, or indirect contact by use of a mechanically conducting line to guide the pressure pulse out of the discharge chamber and to the sensor. In the present application the choice is effectively limited to the direct contact probe because of the desired precise correlation of pressure patterns with those of current and luminosity; thus the noise discrimination problem must be met at its worst.

The principles of operation of a piezoelectric transducer are well known and will not be repeated here. The design of the particular transducer used here is sketched in Fig. 7. A piezoelectric disc (PZT-5, Clevite Corp.) is attached to a backing rod with similar acoustic properties (e.g., brass) using Eccobond conducting epoxy. Silver paint serves as the top electrode, connecting the crystal to the outer brass cylinder. A few layers of Zapon lacquer are sufficient to shield the probe electrically for a few discharges, after which new coatings must be added. The complete unit is inserted in a nylon fitting for mounting in the discharge chamber. The response of the transducers is calibrated by testing them in the end wall of a small shock tube, where they are subjected to head-on reflection of the shock wave. A typical oscillograph response to such a test is shown in Fig. 8. It is evident that the pressure profile is not faithfully preserved, but the first rising pulse is sufficiently fast (approx. 0.1 μsec) to locate the arrival of a pulse within 0.2 μsec as desired in the discharge application.

With this understanding of the gauge response, the probe was exposed to a series of discharges in the 8" diameter pinch

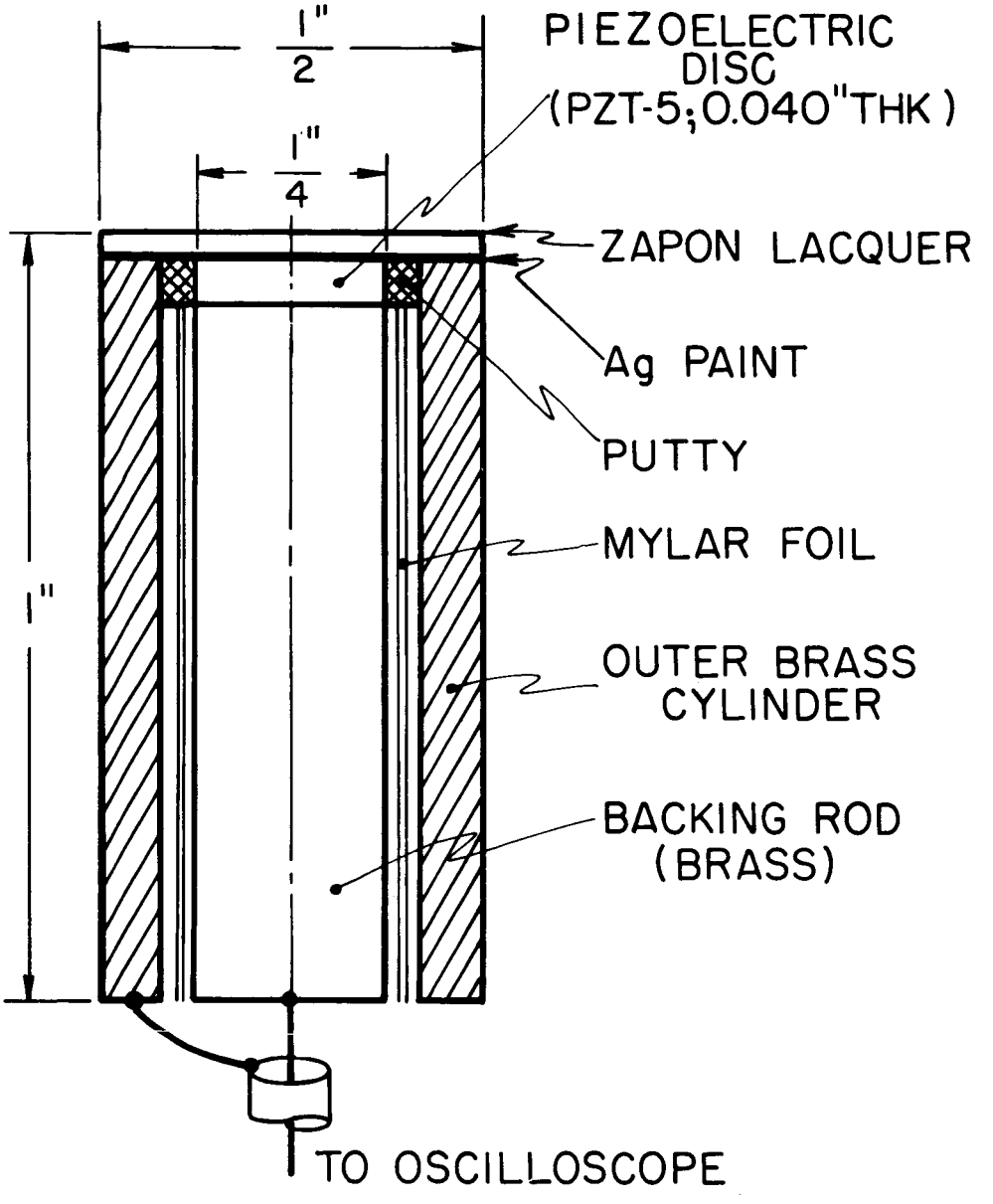

PIEZOELECTRIC PRESSURE PROBE (SCHEMATIC)

AP25-4096-66

FIGURE 7

AP25-P46-66

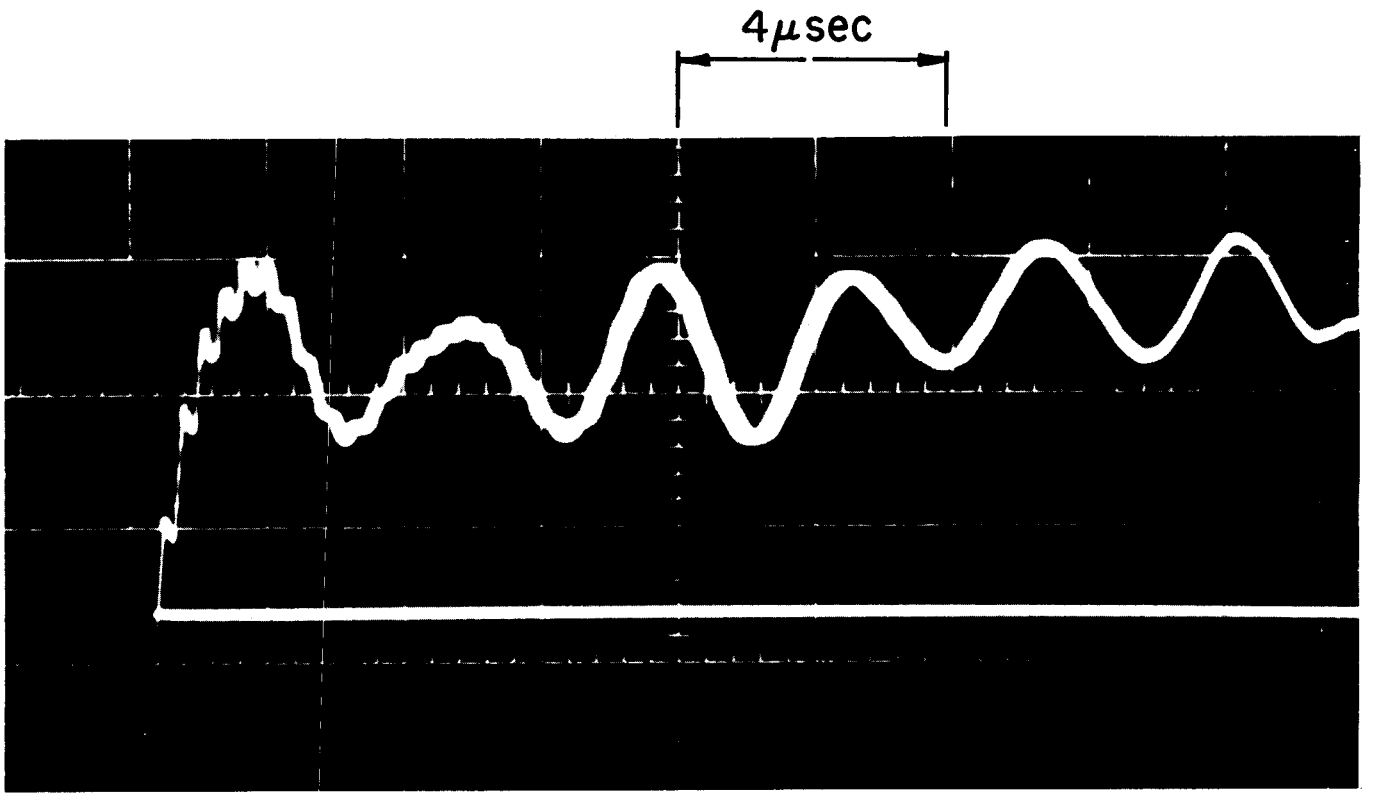

RESPONSE OF PIEZOELECTRIC PROBE TO REFLECTED SHOCK WAVE IN SHOCK TUBE

FIGURE 8

chamber, driven by a pulse-forming network providing a 5 μsec rectangular waveform. With the probe surface flush with the electrode wall, the gradient and magnitude of the passing pressure pulse was observed to increase as the pinch approached the center of the chamber (Fig. 9a). With a modified probe set on a nylon mounting fixture so as to face the incoming pinch head-on, similar results were obtained, but the responses were of greater magnitude because of the associated stagnation effects (Fig. 9b).

In a separate series of experiments, a $\dot{B}$ probe was fastened rigidly adjacent to the pressure probe to obtain precise correlation of the arrival of the current sheet and pressure front. It was observed that the pressure pulse arrives noticeably after the $\dot{B}$ peak (Fig. 10). This separation of current sheet and pressure front has been observed by other investigators[II-2,3] and has profound implications for the model of the gas sweeping process. For example, it immediately confuses all concepts of a current "piston" driving a gasdynamic shock, since the shock in this observation trails the "piston".

Before pursuing this observation in greater detail, it seems worthwhile to attempt development of a transducer which has not only the necessary rise time, but also reproduces the later details of the pressure pulse more faithfully. It is apparent from probe responses such as Fig. 8 that two types of crystal oscillation are occurring: 1) short period oscillations (approx. 0.2 μsec) apparently due to thickness vibrations, and 2) long period oscillations (approx. 2 μsec) apparently due to radial oscillations; obviously both modes are undesirable. The thickness oscillation mode can be attributed to the inability of the axial stress wave to propagate completely out of the crystal because a component is reflected back at the crystal-backing rod interface and then oscillates within the crystal. Ideally, if the crystal and backing rod were perfectly matched there would be no reflection, but with a bonding agent and nonuniformities at the interface this is difficult to obtain. The radial oscillation can be attributed to the fact that the crystal is a finite size, three dimensional system and hence a stress application in one direction affects the stress distribution in all directions, i.e. axial stresses induce radial stresses which propagate in a radial mode. Theoretical analysis of either system is difficult, even neglecting the evident interaction of the two modes to produce a more complex behavior. Systematic variation of several factors that would affect the probe response has been performed experimentally and each has been found to have a critical effect. Specifically: the thickness of silver paint for the electrode has an optimum value; the type of material at the sides of the crystal severely affects the radial oscillation; the relative

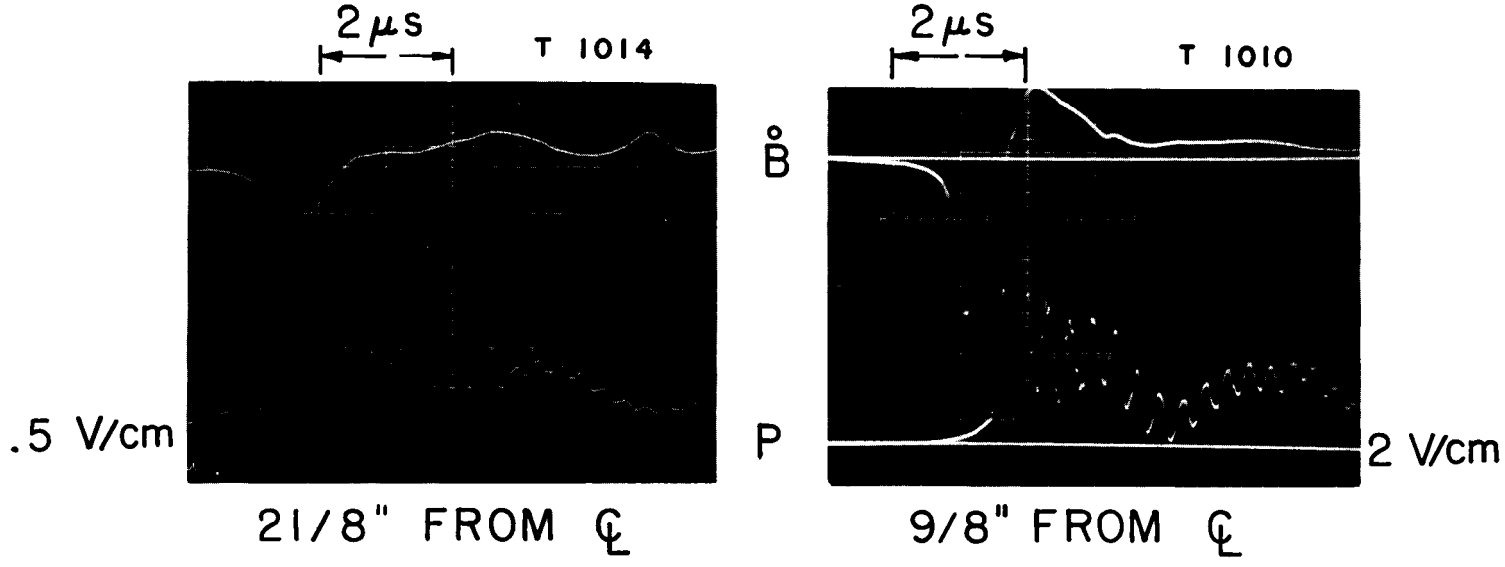

a) PROBE FACE IN PLANE OF ELECTRODE

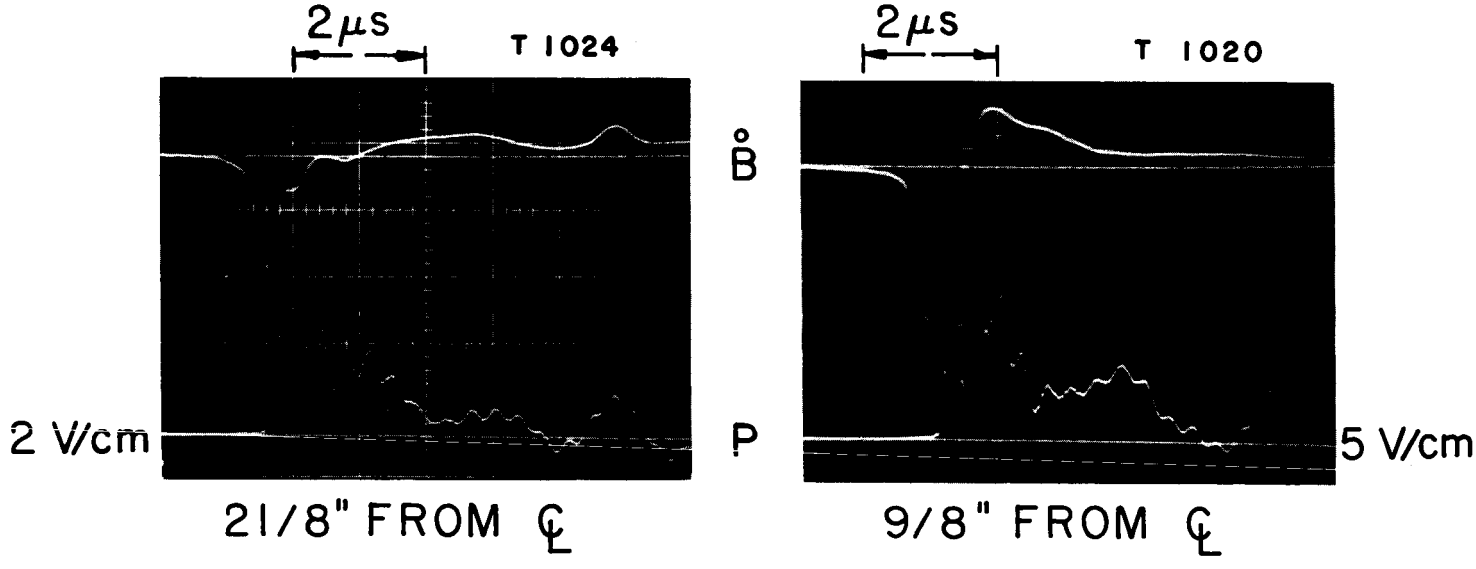

b) PROBE FACING THE DISCHARGE IN MIDDLE OF CHAMBER

RESPONSE OF PIEZOELECTRIC PROBE TO DISCHARGE IN T-PINCH APPARATUS

FIGURE 9

AP25-P45-66

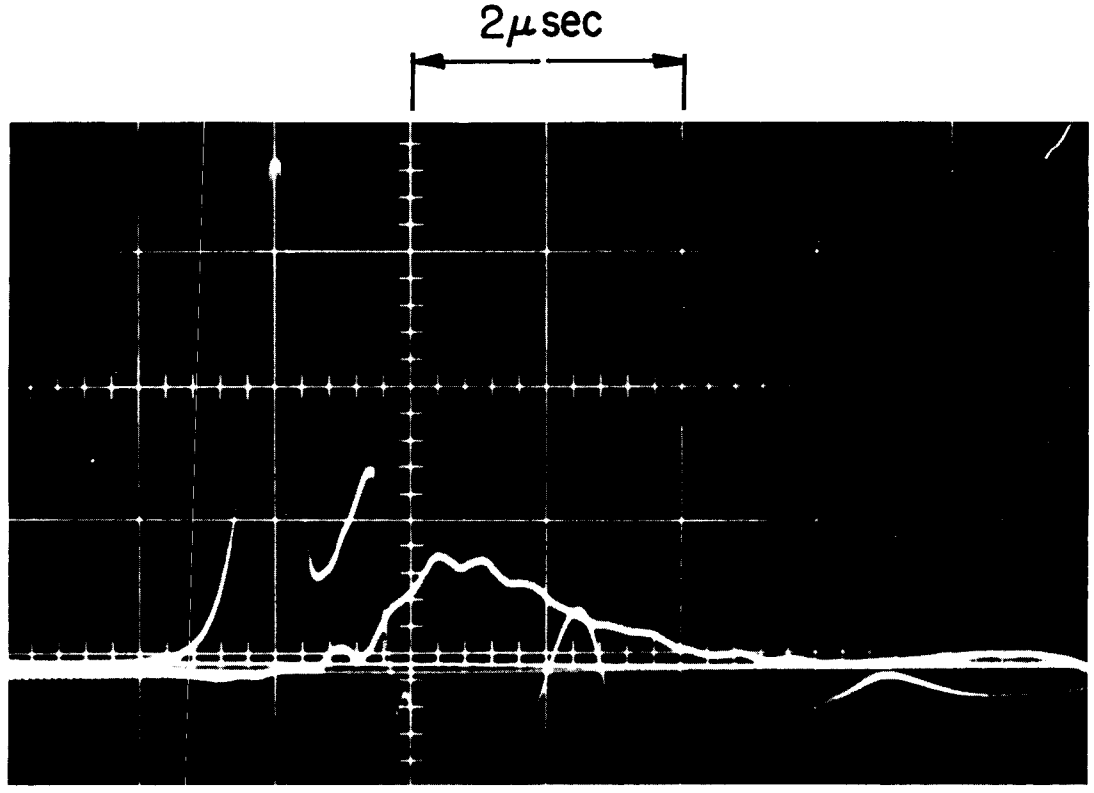

CORRELATION OF HEAD-ON PRESSURE PROBE AND MAGNETIC PROBE RESPONSES 3/4" FROM AXIS IN MIDDLE OF CHAMBER

FIGURE 10

diameter of the crystal-backing rod directly affects the radial oscillations; the acoustic match between crystal-backing rod bears on the axial oscillations; the crystal thickness directly affects the rise time characteristics.

These empirical studies continue in an attempt to develop an optimum configuration for the present application. At this point it appears that the relative time of arrival of the pressure pulse can be accurately determined, and that at least approximate values can be deduced for the magnitude of the initial pressure pulse. Accurate determination of the history of pressure with time appears far more challenging, and will hinge on controlling the spurious crystal oscillations.

IV. MICROWAVE PROBING OF CLOSED CHAMBER DISCHARGES (Ellis)

Microwave studies have been carried out to determine some of the free electron properties of argon and helium discharges in the 8" diameter pinch device. Information is currently being gathered on electron density distributions as a function of position and time throughout the discharge, the magnitude of electron-neutral and electron-ion collision frequencies, and the inhomogeneity and asymmetry of the plasma in the vicinity of the electrodes. This information is essential to complete understanding of the acceleration process, and microwave techniques are especially attractive because they introduce minimal disturbances into the plasma under study.

Microwave studies previously reported have dealt with the determination of electron densities by the reflected amplitude method.[I-14,21] These experiments have shown that the extremely high electron densities prevailing in the current sheet region and the pinch column render conventional microwave techniques ineffective over much of the time regime of interest. At a typical initial pressure of 120 μ in argon, for example, maximum densities of the order of 10^{17} electrons per cubic centimeter appear to exist in the pinch column. This is three orders of magnitude above the critical or "cutoff" density of 10^{14} for the 4 mm. microwave equipment at hand, making detailed information on electron density distributions difficult to obtain.

In order to overcome this difficulty, a new microwave probing technique has been developed which makes use of an interferometer arrangement to determine the phase angle of the reflected wave. The phase information thus obtained can be related to the electron density at the position of the probe by the following analysis.

Consider a plane, linearly polarized electromagnetic wave of frequency ω, incident upon a plasma interface, as shown in Fig. 11. By applying the boundary conditions indicated in Fig. 11 to the incident, reflected, and transmitted wave trains, the complex reflection coefficient can be evaluated in the usual way.[II-4] In polar form,

$$R = \frac{E_i}{E_r} = \left| R \right| e^{i\varphi_r} \qquad (1)$$

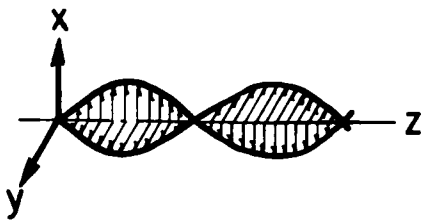

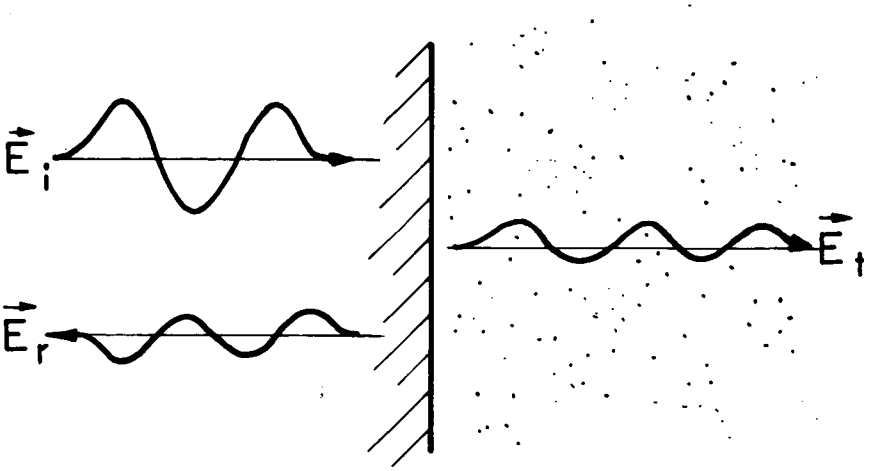

1 – THE INCIDENT WAVE :

$$\begin{cases} \vec{E}_i(z,t) = E_1^+ e^{i(\omega t - k_1 z)} \hat{x} \\ \vec{H}_i(z,t) = H_1^+ e^{i(\omega t - k_1 z)} \hat{y} \end{cases}$$

2 – THE REFLECTED WAVE :

$$\begin{cases} \vec{E}_r(z,t) = E_1^- e^{i(\omega t + k_1 z)} \hat{x} \\ \vec{H}_r(z,t) = H_1^- e^{i(\omega t + k_1 z)} \hat{y} \end{cases}$$

3 – THE TRANSMITTED WAVE:

$$\begin{cases} \vec{E}_t(z,t) = E_2^+ e^{i(\omega t - k_2 z)} \hat{x} \\ \vec{H}_t(z,t) = H_2^+ e^{i(\omega t - k_2 z)} \hat{y} \end{cases}$$

THE ELECTROMAGNETIC BOUNDARY CONDITIONS AT AN INTERFACE REQUIRE THAT :

$$E_i(o,t) + E_r(o,t) = E_t(o,t)$$

$$H_i(o,t) + H_r(o,t) = H_t(o,t)$$

SLAB MODEL FOR MICROWAVE DIAGNOSTIC EXPERIMENTS

JPR2345

FIGURE 11

where $|R| = \dfrac{\left[\left(k_1^2 - \alpha^2 - \beta^2\right)^2 + 4 k_1^2 \beta^2\right]^{1/2}}{(k_1 + \quad)^2 + \beta^2}$ (2)

$$\varphi_r = \tan^{-1}\left[\frac{2k_1 \beta}{k_1^2 - \quad^2 - \beta^2}\right] \tag{3}$$

with the definitions:

$k_1 = \dfrac{\omega}{c}$ = propagation coefficient for free space

$k_2 = \alpha - i\beta$ = complex propagation coefficient of the plasma

c = vacuum velocity of light

Here α and β are lengthy functions of the electron density n (through the plasma frequency, $\omega_p^2 = \dfrac{ne^2}{\epsilon m}$) and the effective collision frequency ν_c characterizing the plasma

$$\alpha = \frac{k_1}{\sqrt{2}}\left[\left(1 - \frac{(\omega_p/\omega)^2}{1+(\nu_c/\omega)^2}\right) + \left\{\left[1 - \frac{(\omega_p/\omega)^2}{1+(\nu_c/\omega)^2}\right]^2 + \left[\frac{(\omega_p/\omega)^2}{1+(\nu_c/\omega)^2}\right]^2\left(\frac{\nu_c}{\omega}\right)^2\right\}^{1/2}\right]^{1/2} \tag{4}$$

$$\beta = \frac{k_1}{\sqrt{2}}\left[-\left(1 - \frac{(\omega_p/\omega)^2}{1+(\nu_c/\omega)^2}\right) + \left\{\left[1 - \frac{(\omega_p/\omega)^2}{1+(\nu_c/\omega)^2}\right]^2 + \left[\frac{(\omega_p/\omega)^2}{1+(\nu_c/\omega)^2}\right]^2\left(\frac{\nu_c}{\omega}\right)^2\right\}^{1/2}\right]^{1/2} \tag{5}$$

At the probing frequency ($\omega = 4.4 \times 10^{11}$ sec^{-1}) electron collisions are relatively infrequent, $\dfrac{\nu_c}{\omega} << 1$. Plots of $|R|$ and φ_r as functions of the electron density for the collisionless case, $\nu_c/\omega = 0$, are displayed in Fig. 12. Here it is seen that, although $|R|$ is unresponsive to changes in n above the critical value, the phase φ_r undergoes a shift of 180°, over the range $1.0 < n/n_c < 10^3$.

AP25-4094-66

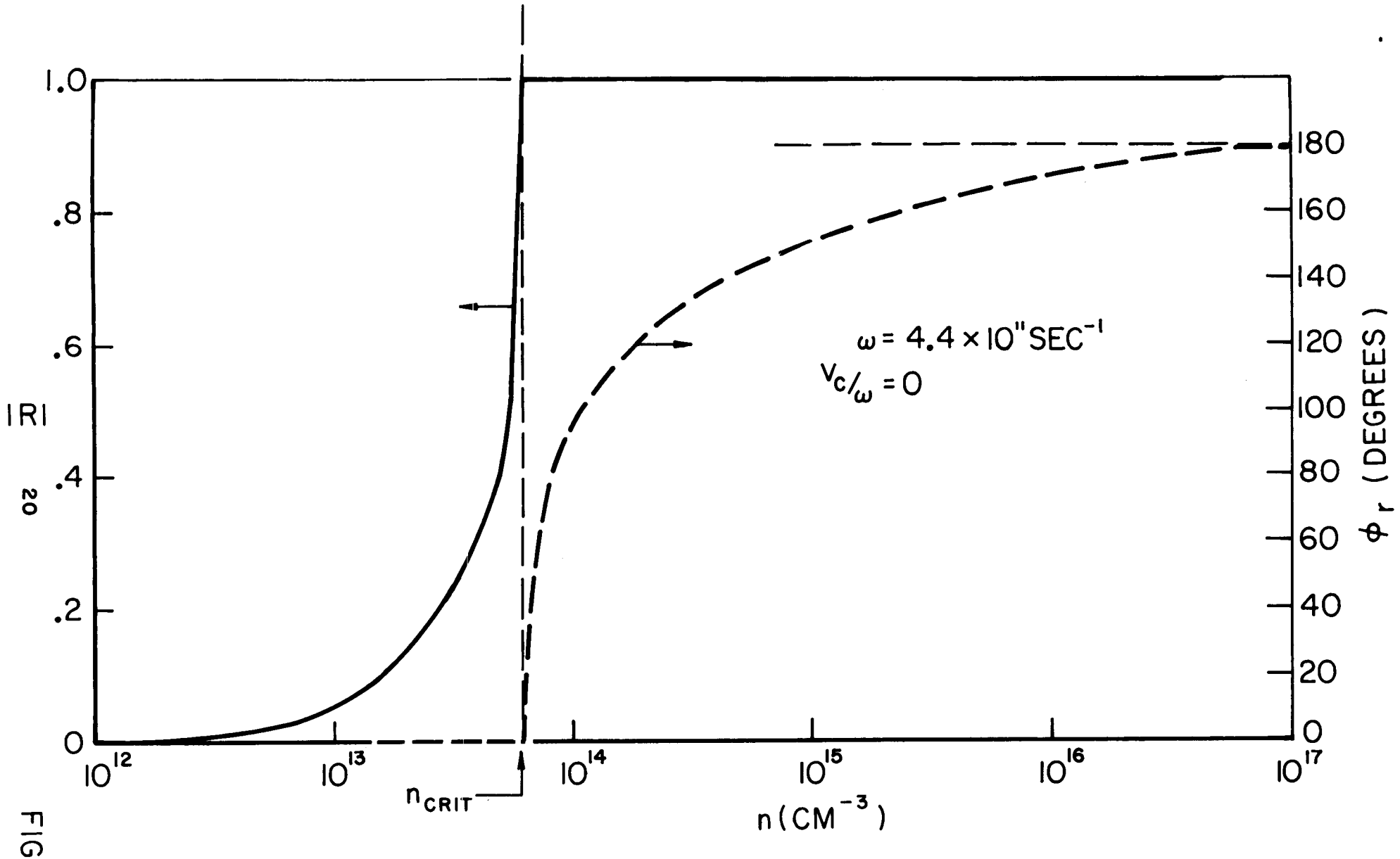

FIGURE 12

REFLECTED AMPLITUDE AND PHASE AS FUNCTIONS OF ELECTRON DENSITY

To measure this phase shift we employ an interferometer, sketched schematically in Fig. 13 which will respond to the resultant of the reflected wave of changing phase and a reference signal from another part of the circuit. Using a square law detector, the response of the circuit to electron density is shown in Fig. 14. The range of measurement is seen to be extended to densities far above the critical value, for a variety of collision frequencies. The great sensitivity of the cusp heights to collision frequencies suggests a relatively simple method for inferring electron collision frequencies.

The above method must be used with considerable caution, however. Because it is inherently limited to produce only a single fringe (180^{o} phase shift), the reflected phase interferometer is critically sensitive to the diffuseness of the reflecting plasma boundary. Any plasma inhomogeneities on the scale of a wavelength (4 mm) at the interface will introduce first order corrections into electron density measurements based on this method. A careful study of this problem has led to the development of a wave propagation theory for lossy plasmas in which severe charged species density gradients are present. If an exponential variation of electron density of the form $n(z) = n_{\infty}[1-e^{-2m(z/\lambda_o)}]$ exists near the boundary, for example, (Fig. 15) the complex reflection coefficient can be shown to take the form

$$R = \frac{(1+K)\,J_p(x) + i\sqrt{1-K^2}\,J_{p-1}(x)}{(1-K)\,J_p(x) - i\sqrt{1-K^2}\,J_{p-1}(x)} \qquad (6)$$

where $$K = \frac{k_2}{k_1} = \alpha/k_1 - i\,\beta/k_1 \qquad (7)$$

$J_p(x)$ = 1st kind Bessel function of order p and argument x

$$p = i\,\frac{2\pi}{m}\,K \qquad (8)$$

$$x = \frac{2\pi}{m}\sqrt{1-K^2} \qquad (9)$$

m = ramp width parameter appearing in exponential (defined in Fig. 15)

AP25-4091-66

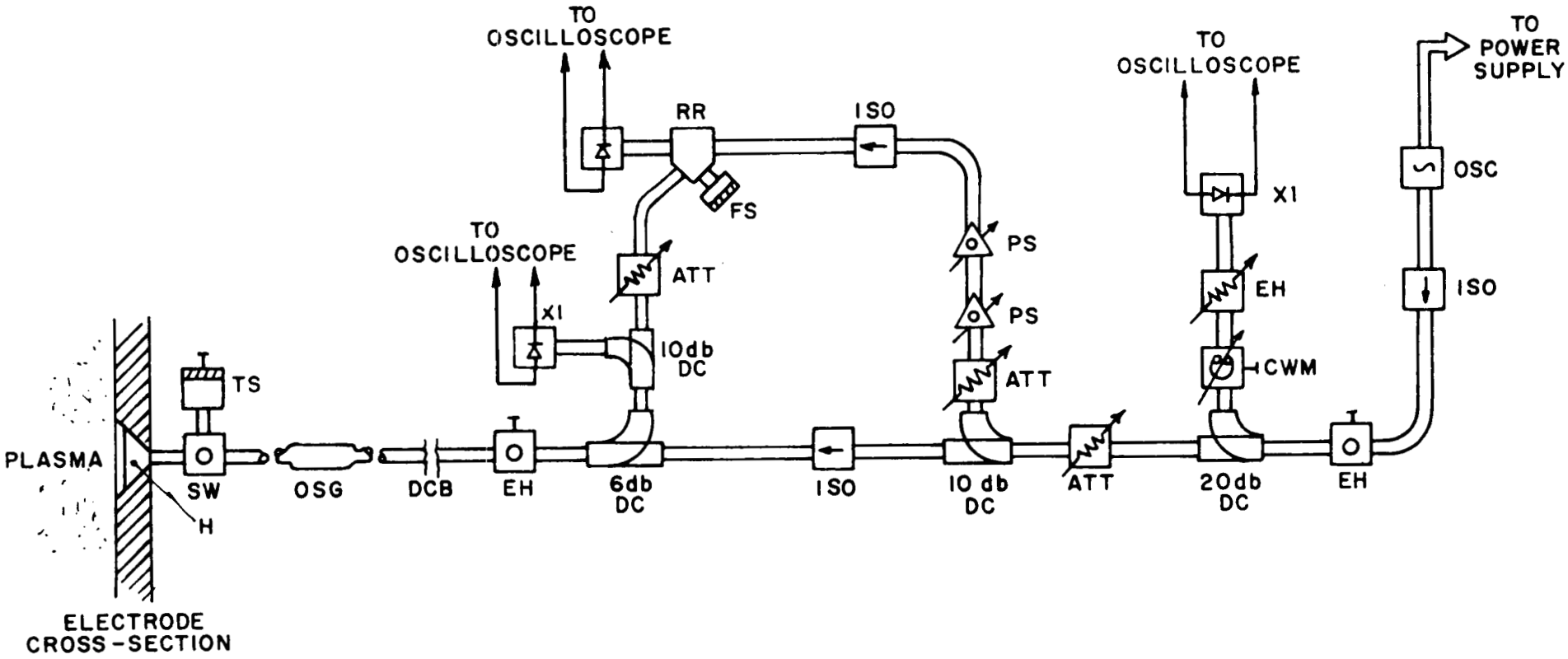

Notation: H, horn; SW, 3-port switch; TS, tunable short; OSG, oversize guide; DCB, direct current break in waveguide; EH, $\overline{E}$ and $\overline{H}$ plane tuner; DC, directional coupler; ATT, variable attenuator; XL, square-law crystal detector; FS, fixed short; RR, rat race; ISO, isolator; PS, variable phase shifter; CWM, cavity wave meter; OSC, reflex klystron oscillator.

FIGURE 13

DIAGRAM OF REFLECTED PHASE INTERFEROMETER

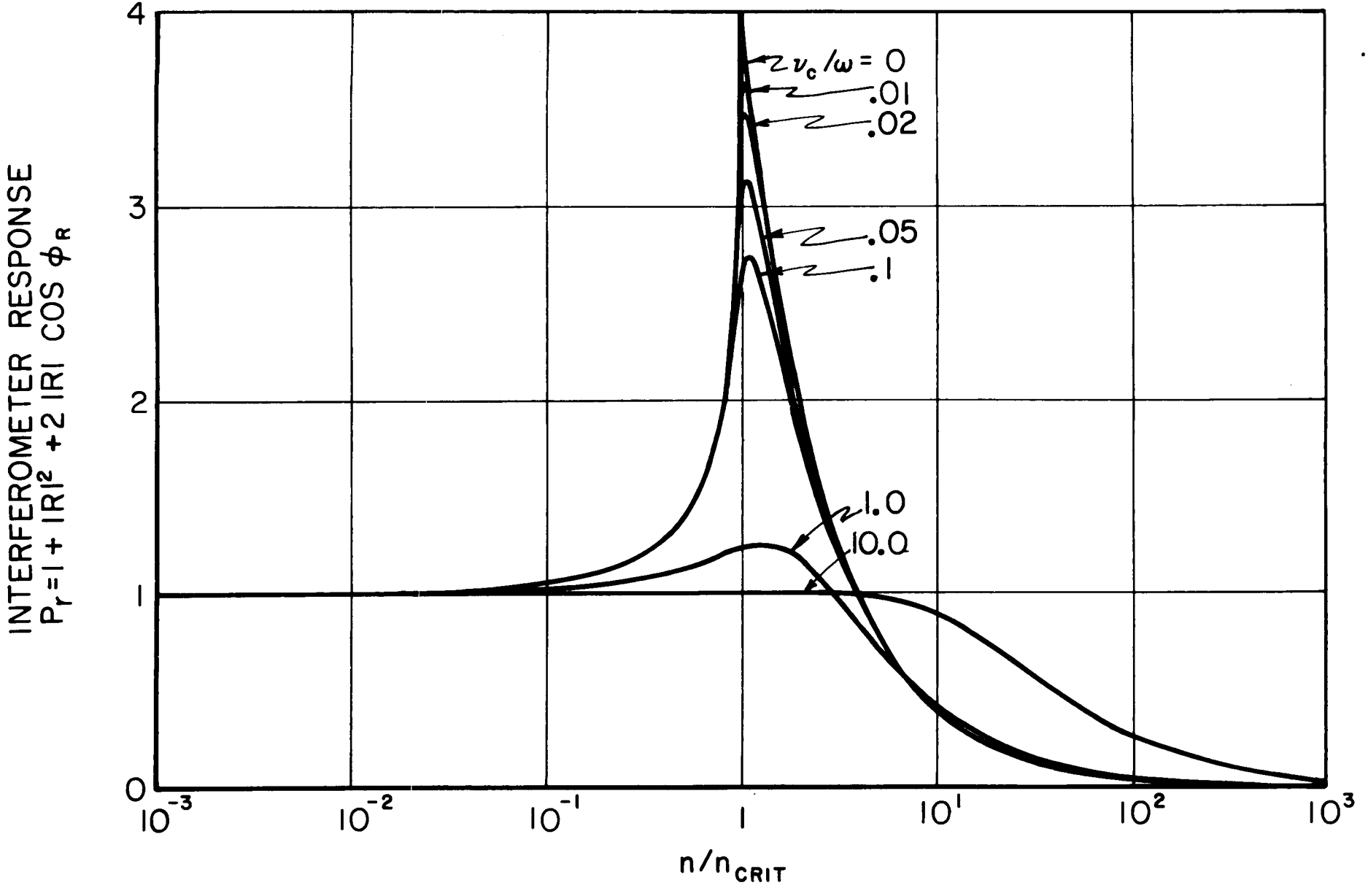

INTERFEROMETER RESPONSE AS FUNCTION OF ELECTRON DENSITY AT SLAB BOUNDARY

FIGURE 14

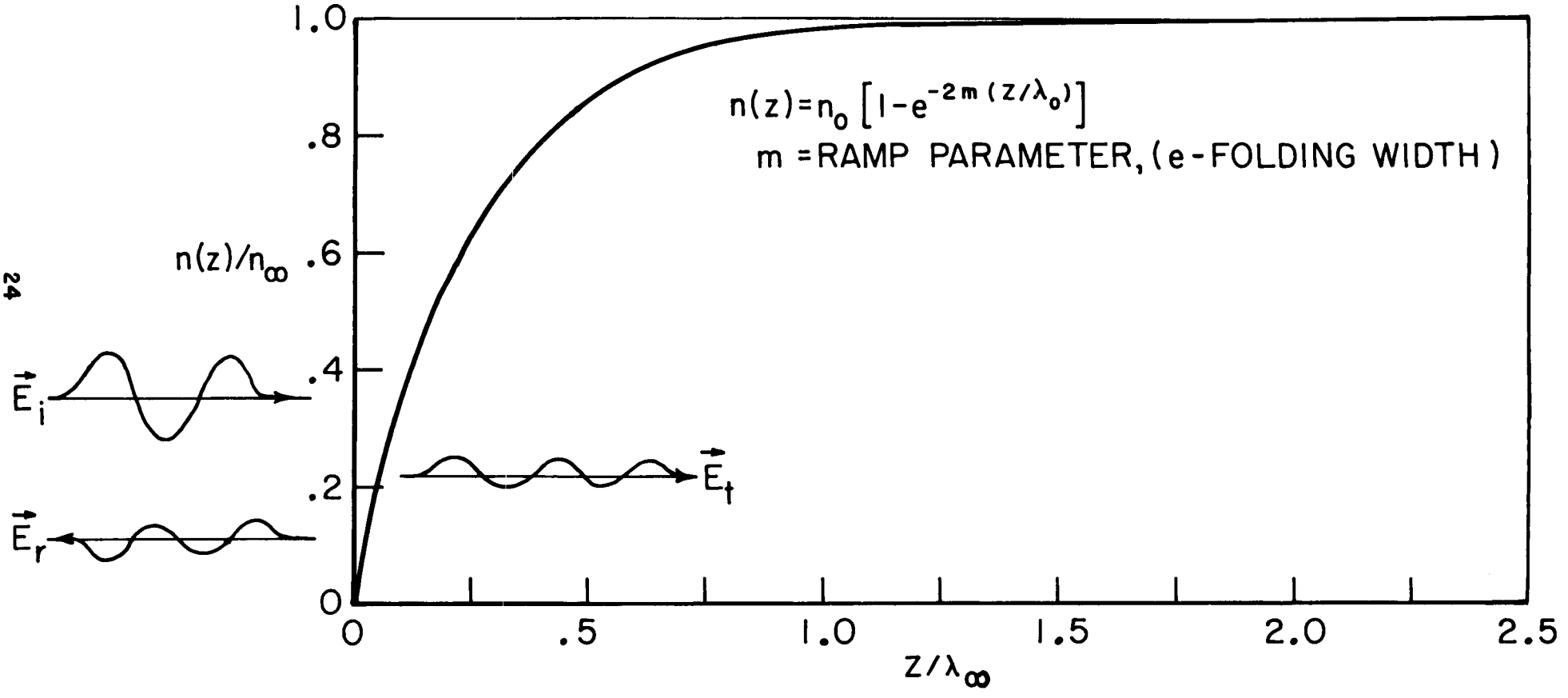

FIGURE 15

EXPONENTIAL RAMP BOUNDARY MODEL FOR MICROWAVE DIAGNOSTIC EXPERIMENTS

Other assumed simple density variations yield equally complicated expressions. Bessel functions of arbitrary complex order and argument do not exist in tabular form, and numerical results for data reduction must be obtained from a computer. Some of these calculations have already been carried out* and others will be done shortly.

The probe itself, including special components and complete instrumentation and shielding facilities has been developed and tested and is now in daily use. Of special interest is the custom horn which has been matched to free space with a voltage standing wave ratio of better than 1.01 by a coated quartz element mounted in its mouth.[I-14,21] A reflected radiation pattern for this horn is shown in Fig. 16. A special upper electrode has been fabricated to accept this horn at various radial positions, as shown in Fig. 17, while maintaining the proper vacuum. Certain waveguide sections of unusual configuration were needed in the bridge circuit of the interferometer (Fig. 18) and were fabricated here with the assistance of the Plasma Physics Laboratory.

A typical oscilloscope trace obtained from the probe during a discharge in 300 μ argon is shown in Fig. 19. The similarity to the theoretical curves in Fig. 14 is evident. Apparently the full regime of electron densities arising in this discharge is now accessible to direct measurement with microwaves. This work will be elaborated and published soon in a separate technical report and in a forthcoming Ph.D. thesis.

*We acknowledge the assistance of the Princeton University and Guggenheim Laboratories Computing Centers in making these numerical computations.

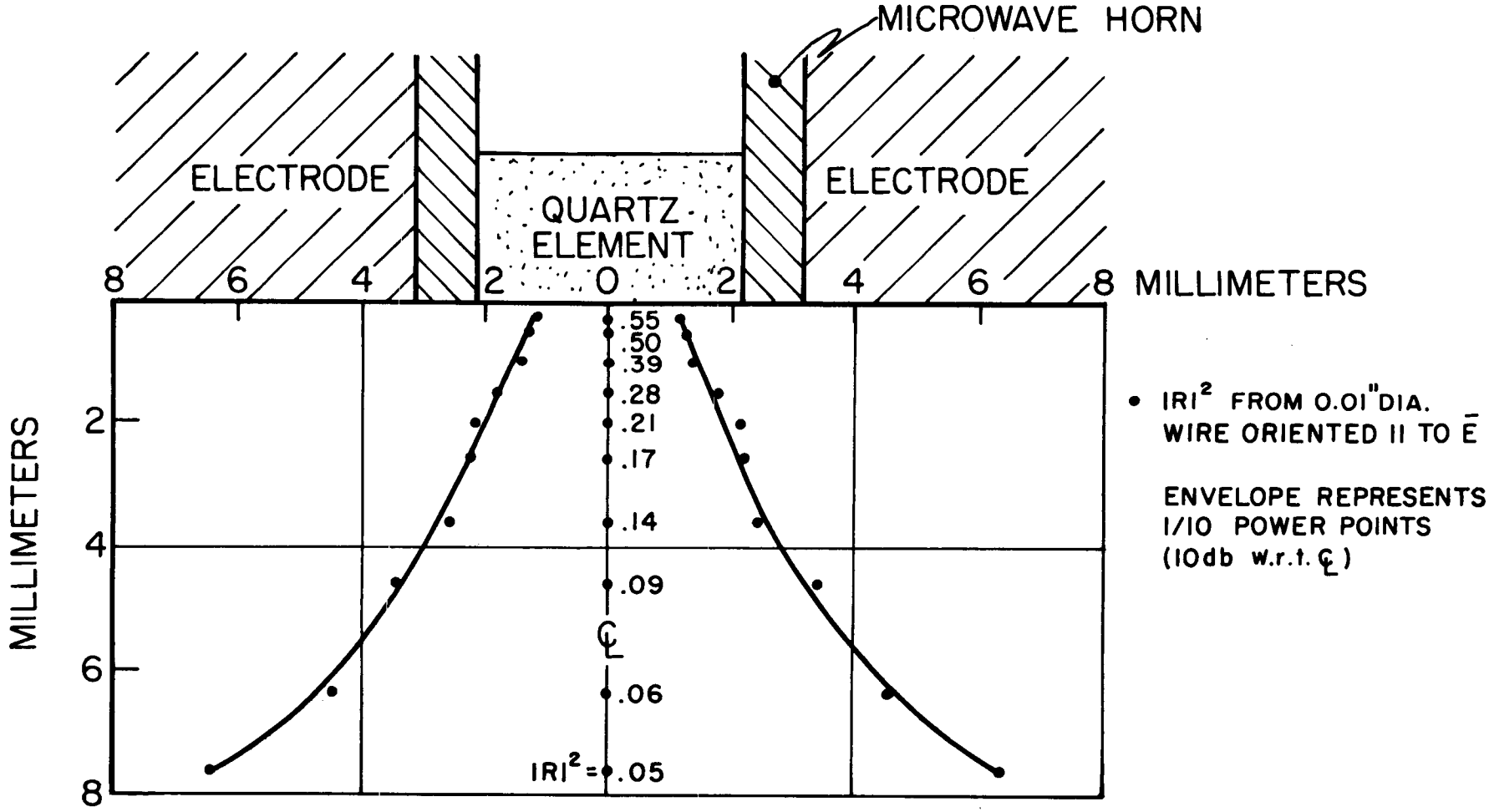

RADIATION PATTERN OF MICROWAVE HORN

FIGURE 16

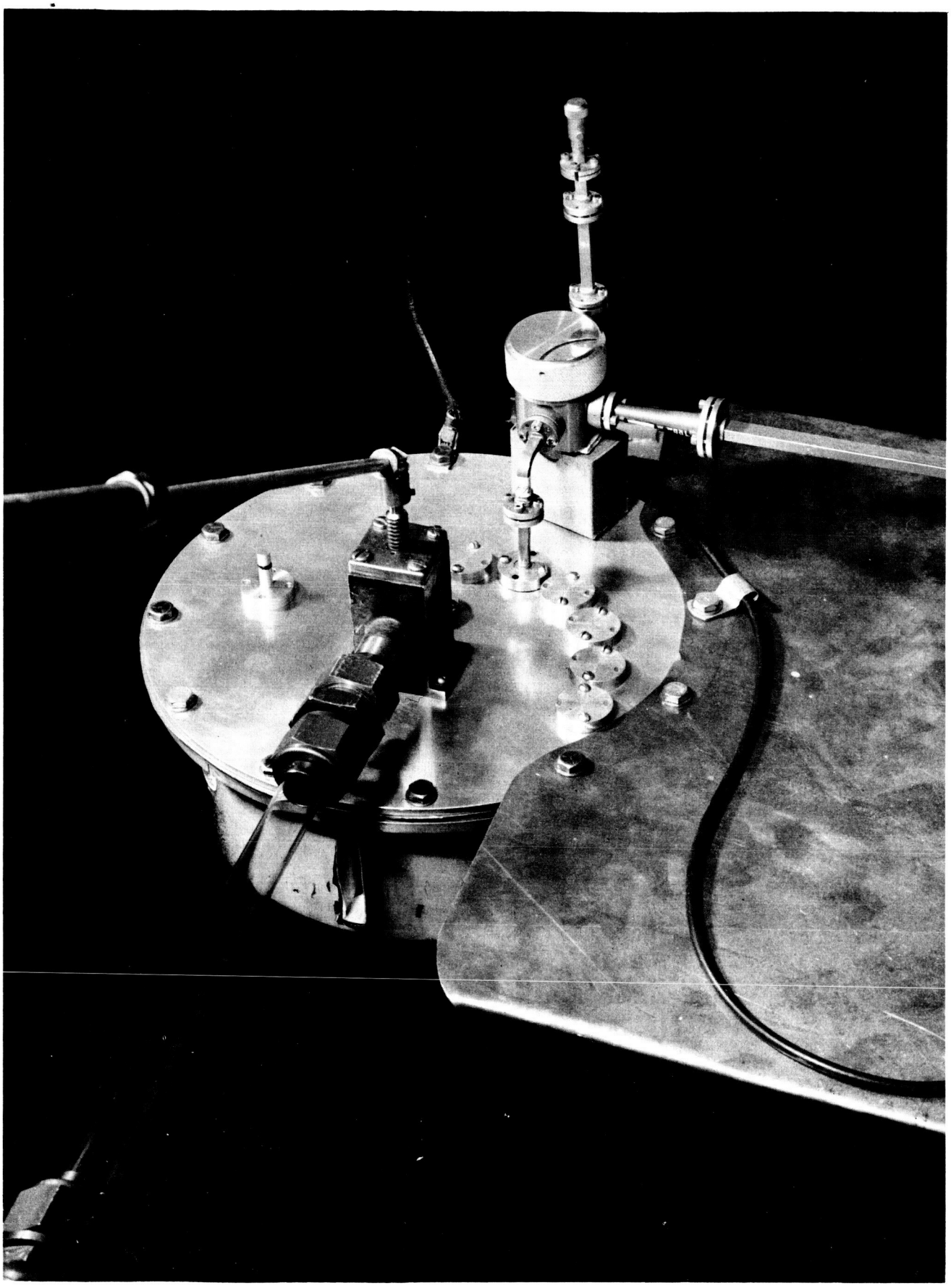

AP25-P40-66

MICROWAVE HORN MOUNTED IN UPPER ELECTRODE OF DISCHARGE CHAMBER

FIGURE 17

AP25-P41-66

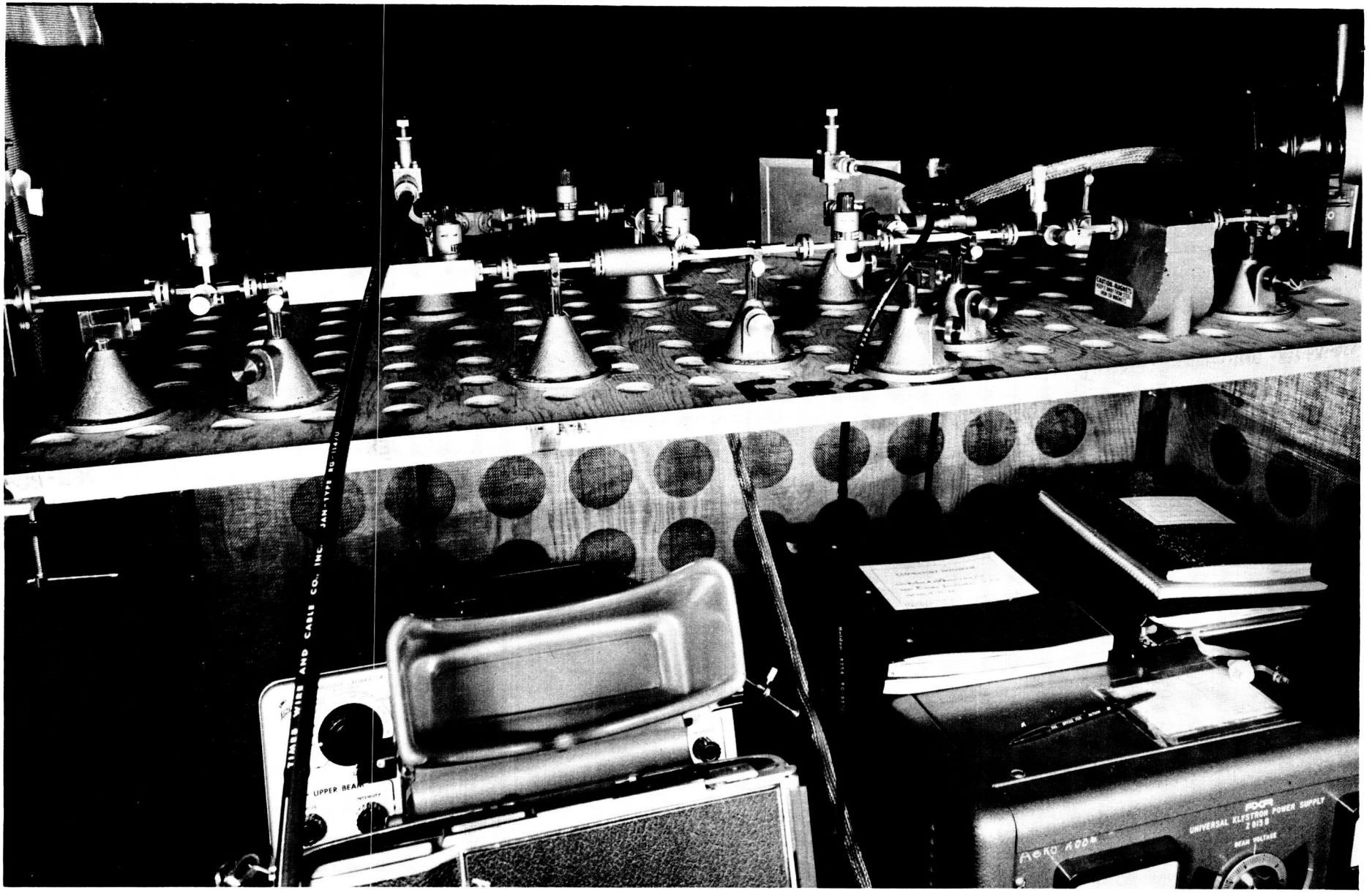

PHOTOGRAPH OF MICROWAVE INTERFEROMETER

FIGURE 18

AP25-P44-66

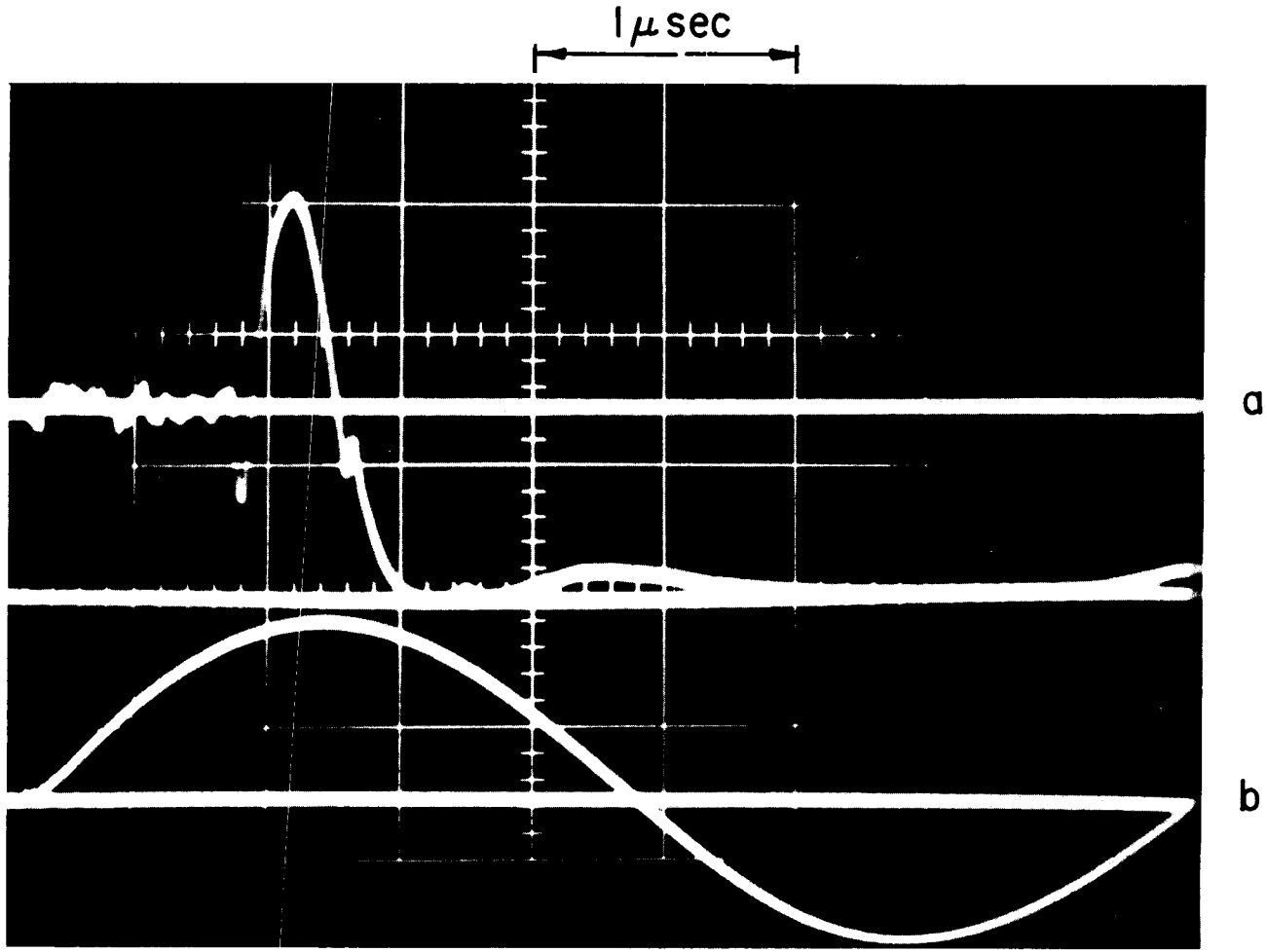

a) INTERFEROMETER ($\lambda_o = 4\,mm$), $\frac{R}{R_o} = 0.5$

b) INTEGRATED ROGOWSKI COIL RESPONSE

RESPONSE OF INTERFEROMETER TO 8" PINCH DISCHARGE IN 300 μ ARGON

FIGURE 19

V. SPONTANEOUSLY BIFURCATING CURRENT SHEETS
(Black)

In the course of systematic study of pinch discharges driven by our tailored-pulse transmission line,[I-14,21,23,24,32] a novel phenomenon has appeared over a narrow range of operating conditions: the inwardly moving current sheet bifurcates when it reaches about one-half radius and thereafter the two components proceed at different velocities. So far this has only been observed at an initial pressure of 100 μ in argon, with a driving current waveform like that shown in Fig. 20. The effect is most directly displayed on unintegrated ($\partial B/\partial t$) magnetic probe records which, in their time dependence are qualitatively similar to the spatial variation of current-density obtained by detailed cross-plotting and graphical differention of a series of integrated (B(t)) records. For example, Fig. 20 displays a $\partial B/\partial t$ record taken at 1.5 inches radius. The double-humped signal seen here can only be generated by two closely spaced propagating current sheets of like sign following each other into the center of the chamber.

In Fig. 21, we have plotted the trajectory of such $\frac{\partial B}{\partial t}$ humps, together with that of the luminous front, derived from streak-camera photographs, and the theoretical snowplow trajectory. A separate point is plotted for each "hump" when bifurcation commences. Over the first half-radius of travel, the (single) humps follow the luminosity front and snowplow trajectory quite closely. When bifurcation occurs, it is the second peak that continues to follow these trajectories; the first hump propagates ahead with greater velocity.

At this time, we have only two clues to the significance of the fore-running pulse. First, its velocity appears to be just twice that of the main front. This brings to mind the two extremes of the opaque-piston concept of plasma acceleration: the snowplow case, in which particles "stick" to the piston, and henceforth move with piston velocity, and the reflecting case, in which particles elastically "bounce off" and thus acquire twice the piston velocity.

Second, we have long searched for the cause of the precursor luminosity which occasionally is seen to arise at the center of the chamber substantially before the arrival of the main luminous front.[I-5] In Fig. 21 we have also indicated the time of occurrence of such precursor luminosity on the centerline from several streak photographs. These points are seen to be reasonable extrapolations of the fore-running $\partial B/\partial t$ hump. This correlation may be spurious, since we have observed

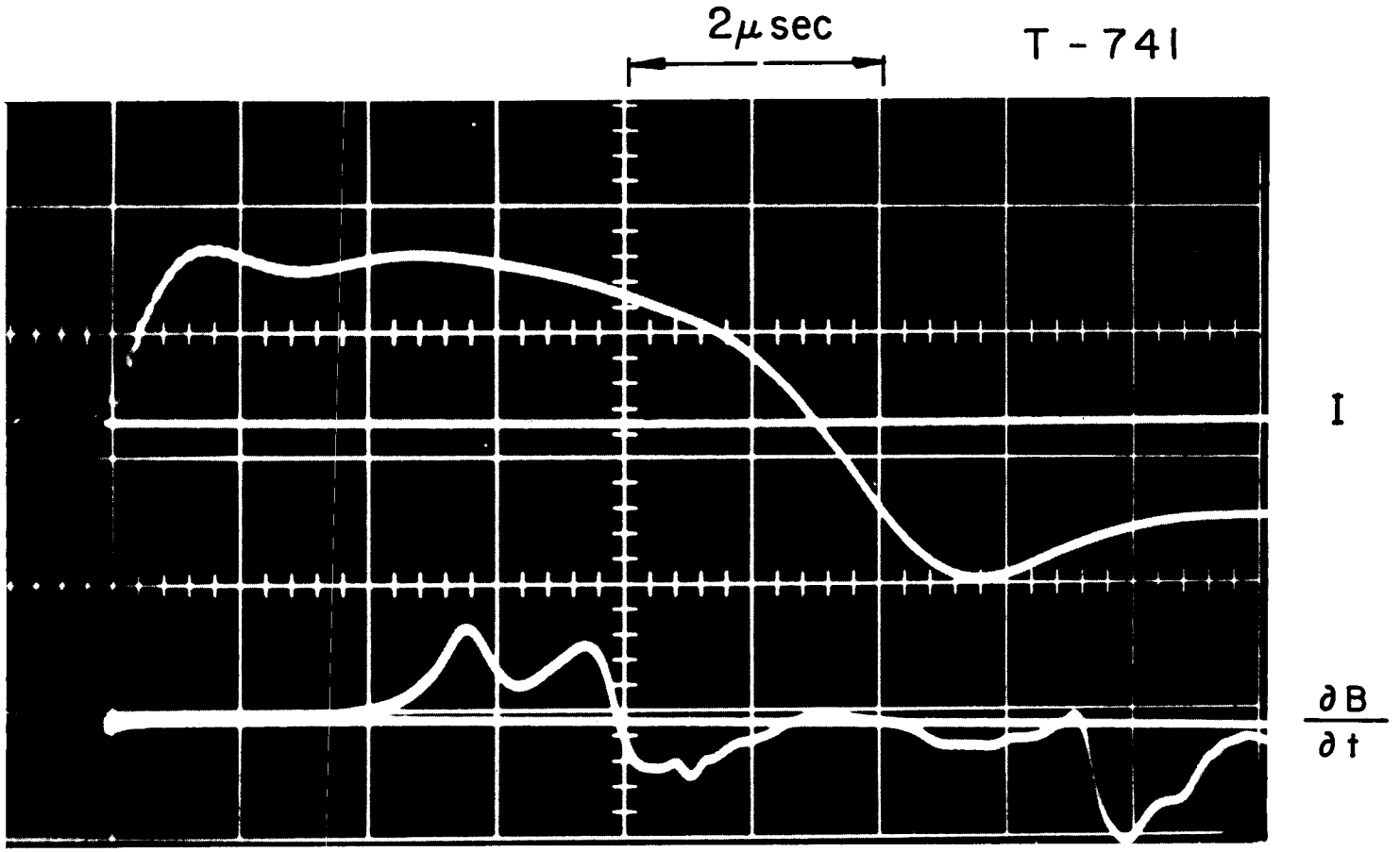

PINCH DISCHARGE CURRENT I AND PROBE RESPONSE
$\partial B/\partial t$, AT R = 1.5"

FIGURE 20

AP25-4099-66

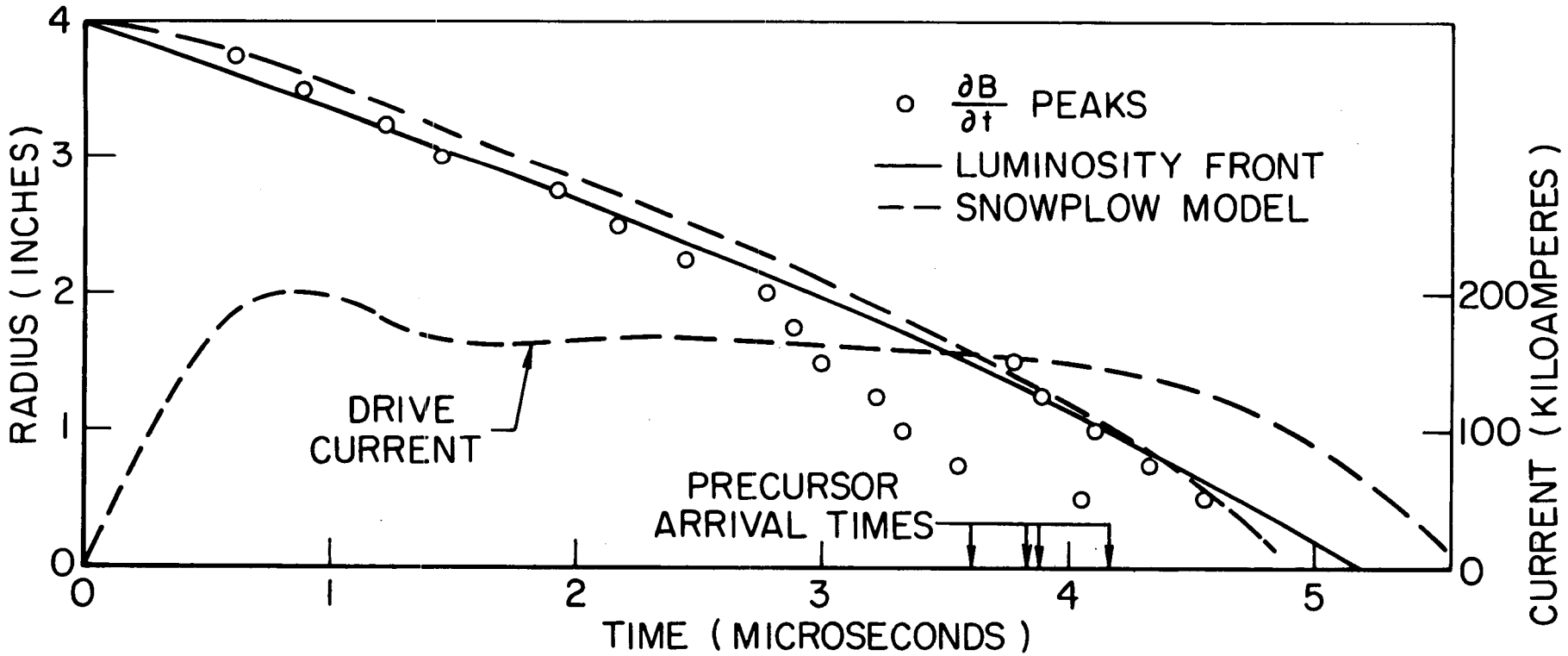

FIGURE 21

TRAJECTORIES OF: $\frac{\partial B}{\partial t}$ MAXIMA, LUMINOUS FRONT AND SNOWPLOW MODEL IN 8" PINCH DISCHARGE AT 100μ ARGON

such precursor luminosity, and even bifurcated luminosity fronts, in cases which show little indication of a bifurcated current distribution.

The identification of the fore-running front will be pursued in the future. One indicated experiment involves the propagation of a pinch into a previously ionized, low pressure gas. Such preionization studies are not difficult, and would provide an environment which should favor the elastic piston behavior mentioned above. If this is indeed the mechanism of the first front, it should be amplified in such an environment. Further details of the current density distributions in the tailored pulse discharges will be presented in a Ph.D. thesis to be submitted shortly.

VI. PLASMA EXHAUST CHARACTERISTICS WITH GAS INJECTION TRIGGERING (Eckbreth)

The two previous semi-annual reports[I-21,29] have dealt in considerable detail with experimental studies of the exhaust of the pinched plasma from an axial orifice. As discussed there, this process is felt to be the single most critical step in the composite pulsed plasma propulsion sequence of physical events, and probably is the dominant factor in the over-all efficiency of devices of this class. During the present reporting period, the work has been expanded in three directions:

1) A 135 μf capacitor bank has been assembled, which can deliver 7 kilojoules of energy when charged to the normal operating voltage of 10,000 volts. This, in conjunction with the pulse-forming techniques previously developed in this laboratory,[I-14,21,23,24,32] is capable of providing rectangular waveforms of widely different characteristics. For example, depending on the magnitude of inter-unit inductance, pulses from 300,000 amperes for 10 μsec, to 3,000 amperes for 800 μsec can be formed. The former extreme overlaps the range of much of our earlier work; the latter extreme is well within the "quasi-steady" regime useful for MPD arc simulation.

2) Magnetic probe studies of the exhaust plume, which lead to contours of enclosed current as a function of time have been applied to exhausts of gas-triggered discharges, which more closely simulate space operation of the accelerator.

3) Ion collecting probes have been constructed to sample the ion flux along the axis of the exhaust plume. From this data, correlation of the gas acceleration phase with the current patterns in the plume are possible.

The largest effort sofar has been devoted to item 2, the mapping of enclosed current contours in the plume as a function of time, for gas-injection triggering. This information was obtained in the conventional way from two 16 turn-2mm., glass-encased magnetic probes inserted at appropriate positions in the field of interest. The resulting current contours are shown in Figs. 22a and 22b. From comparison of these contours with Kerr-cell photographs of the luminous patterns at the corresponding times, one is led to the following conclusions: a) the current contours are more diffuse than the luminous fronts; b) there is a slight lag of the main current zone behind the luminous front trajectory; c) secondary breakdowns do not occur until the pulse reverses regardless of its length over

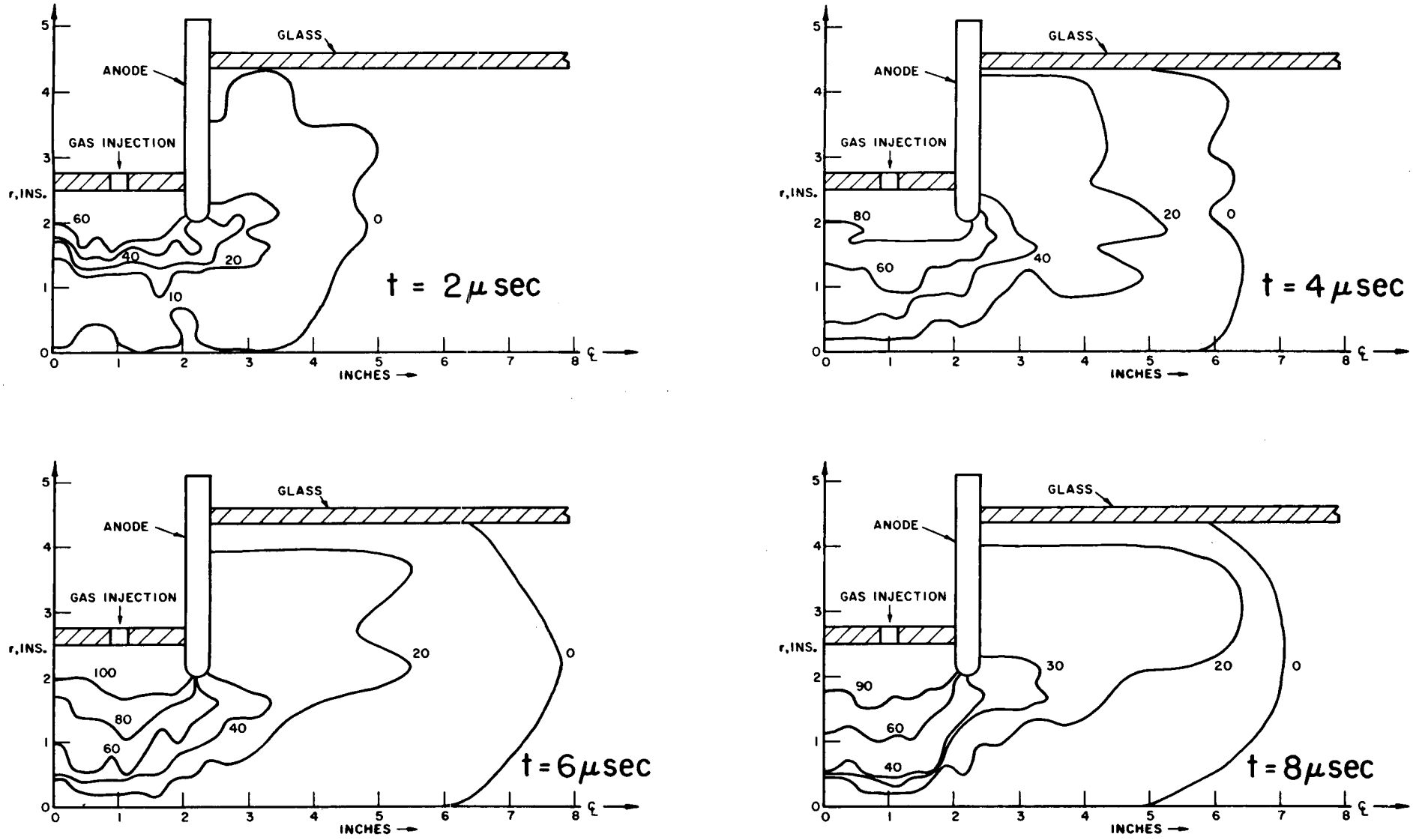

FIGURE 22a

ENCLOSED CURRENT CONTOURS IN A 5" PLASMA PINCH EXHAUST PLUME WITH SHOCK TUBE GAS INJECTION, 120 KA-20μs RECTANGULAR CURRENT WAVEFORM AT: 2, 4, 6, 8 μsec

AP25-R4076-66

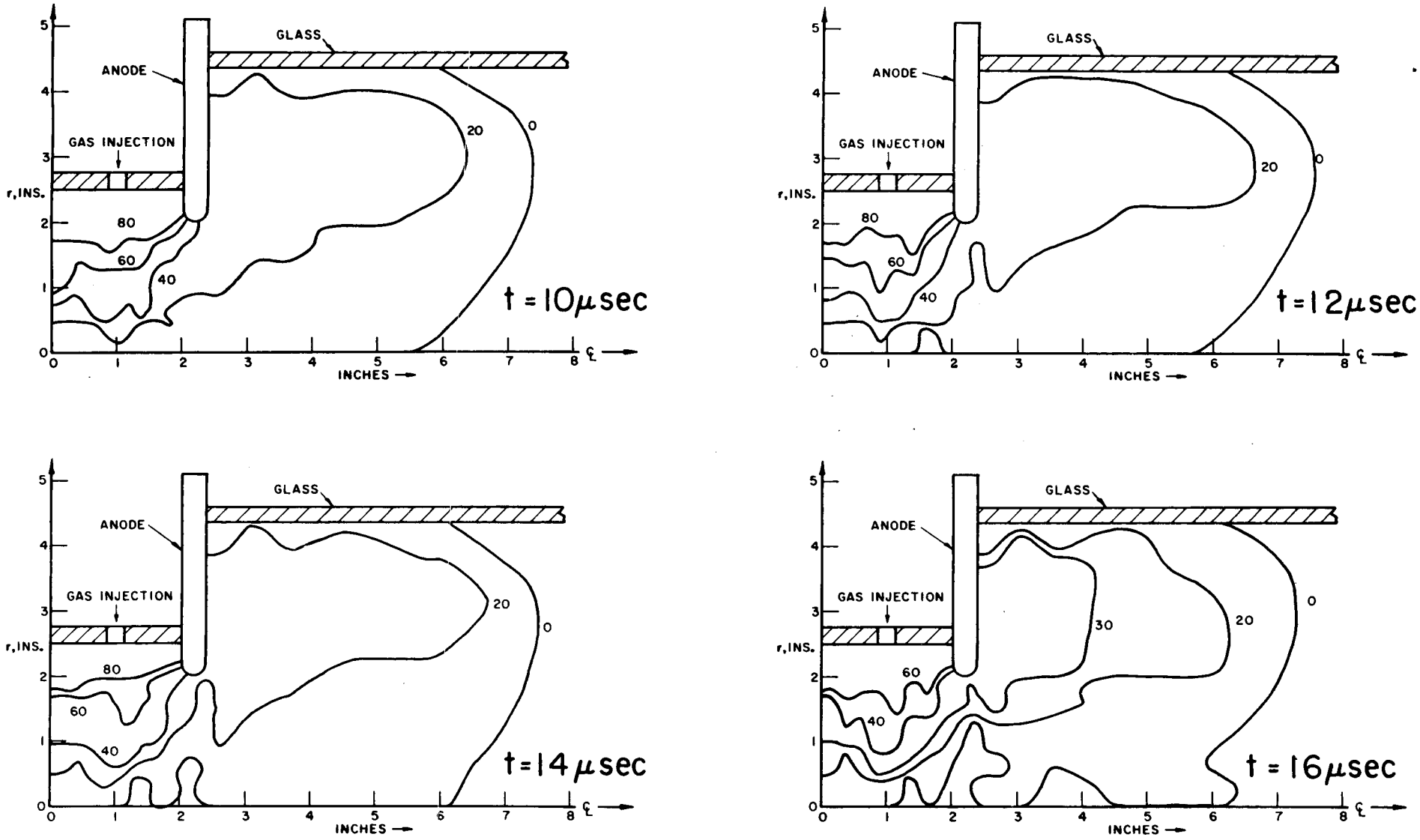

ENCLOSED CURRENT CONTOURS IN A 5" PLASMA PINCH EXHAUST PLUME WITH SHOCK TUBE GAS INJECTION, 120 KA-20μs RECTANGULAR CURRENT WAVEFORM AT: 10, 12, 14, 16μsec

FIGURE 22b

the domain studied; d) the current contours stabilize after about 6 μsec and remain in virtually the same position until the current reverses; e) plume currents are confined within about 4" of the outer electrode; and f) the exhaust vessel appears to confine the exhaust pattern.

The most striking observation, of course, is the stabilization of the current pattern into a steady configuration over the last two-thirds of the 16 μsec pulse. It is of critical importance to determine whether this is a consequence of the constraint imposed by the relatively small exhaust vessel, or a more basic property of the ejection process, and if the latter, whether this stabilization represents a cessation of the useful acceleration phase, or a conversion to a new mode of acceleration akin to the steady flow accelerators. The possibility of exhaust tank interference with the ejection process was the primary motivation for the large Plexiglas vacuum vessel described in Section VIII.

Pending completion of the new vacuum facility, a preliminary series of experiments to monitor the ion flux in the exhaust beam was conducted. The primary aim here was to correlate such ion flux with the observed current configurations in the plume. A conventional Faraday cup probe,[II-5] was inserted from the rear of the exhaust vessel along the axis, as shown in Fig. 23. The probe is negatively biased to repel all electrons and extract ions from the neighboring plasma. A typical trace from this probe is shown in the lower half of Fig. 24. Due to small irreproducibility in the shock tube triggering process, and the close proximity of the probe to the generating area of the plasma, there is some scatter in the observed arrival times of the plasma at the probe. Based on these arrival times and the distances of the probe from the orifice, the plasma velocity over the chamber is found to be approximately 25,000 m/sec. This value is comparable with the original radial motion inside the chamber, again suggesting that the plasma is recovering a significant portion of its radial velocity in axial streaming.[I-21]

It is also to be noted that ion flux continues to be collected long after stabilization of the current pattern has occurred in the plume. This would seem to imply that a new acceleration mechanism has been established after cessation of the more familiar current sheet "sweeping" process. The similarity of the current pattern in this latter phase to that of the steady MPD arc is provocative, and further study of possible transient simulation of the MPD interaction is clearly indicated. Study of longer current pulses, more definitive ion probe experiments, and more detailed current mappings all have been deferred until the availability of the large vacuum vessel.

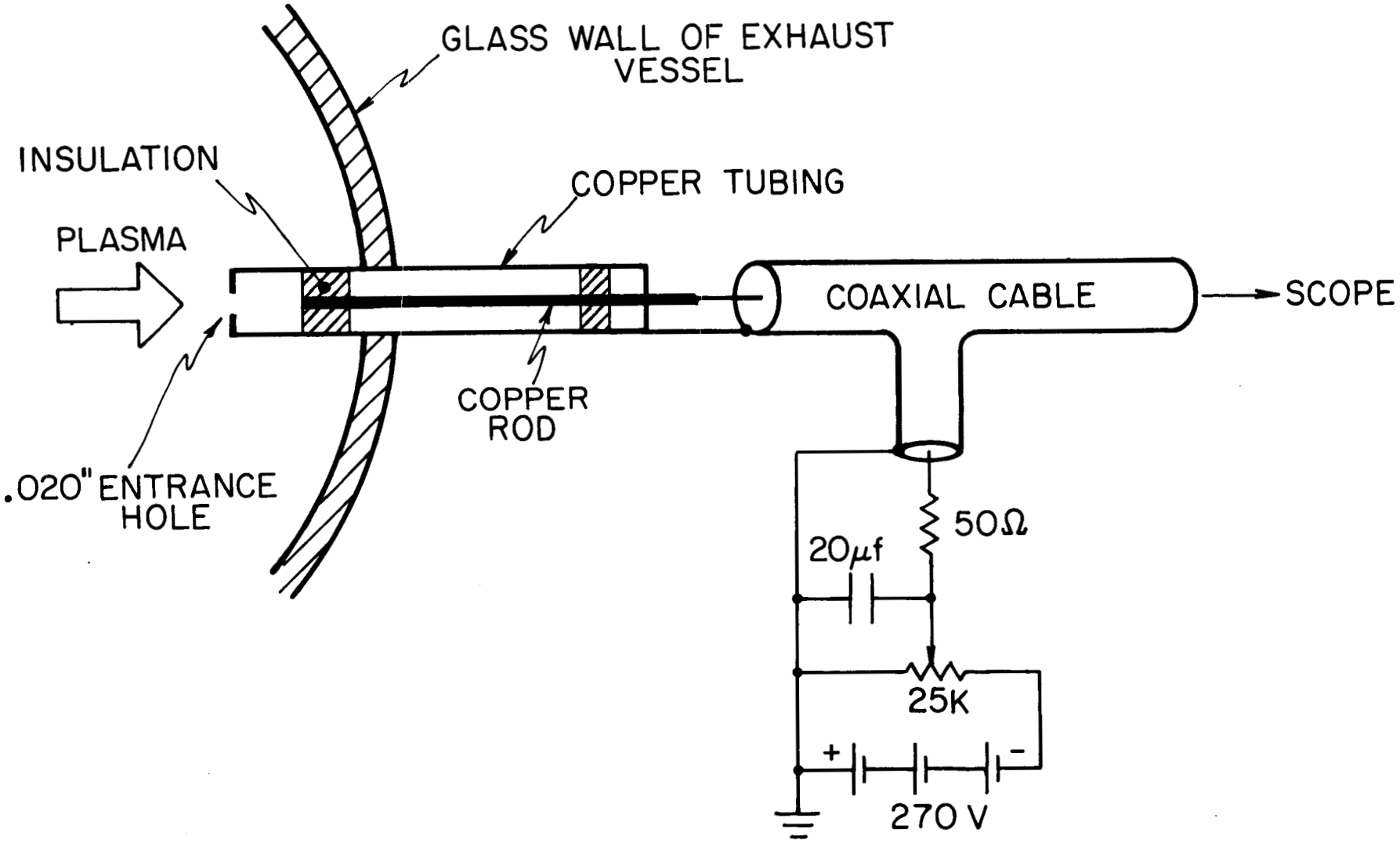

FARADAY CUP PROBE AND BIASING CIRCUIT
(SCHEMATIC)

FIGURE 23

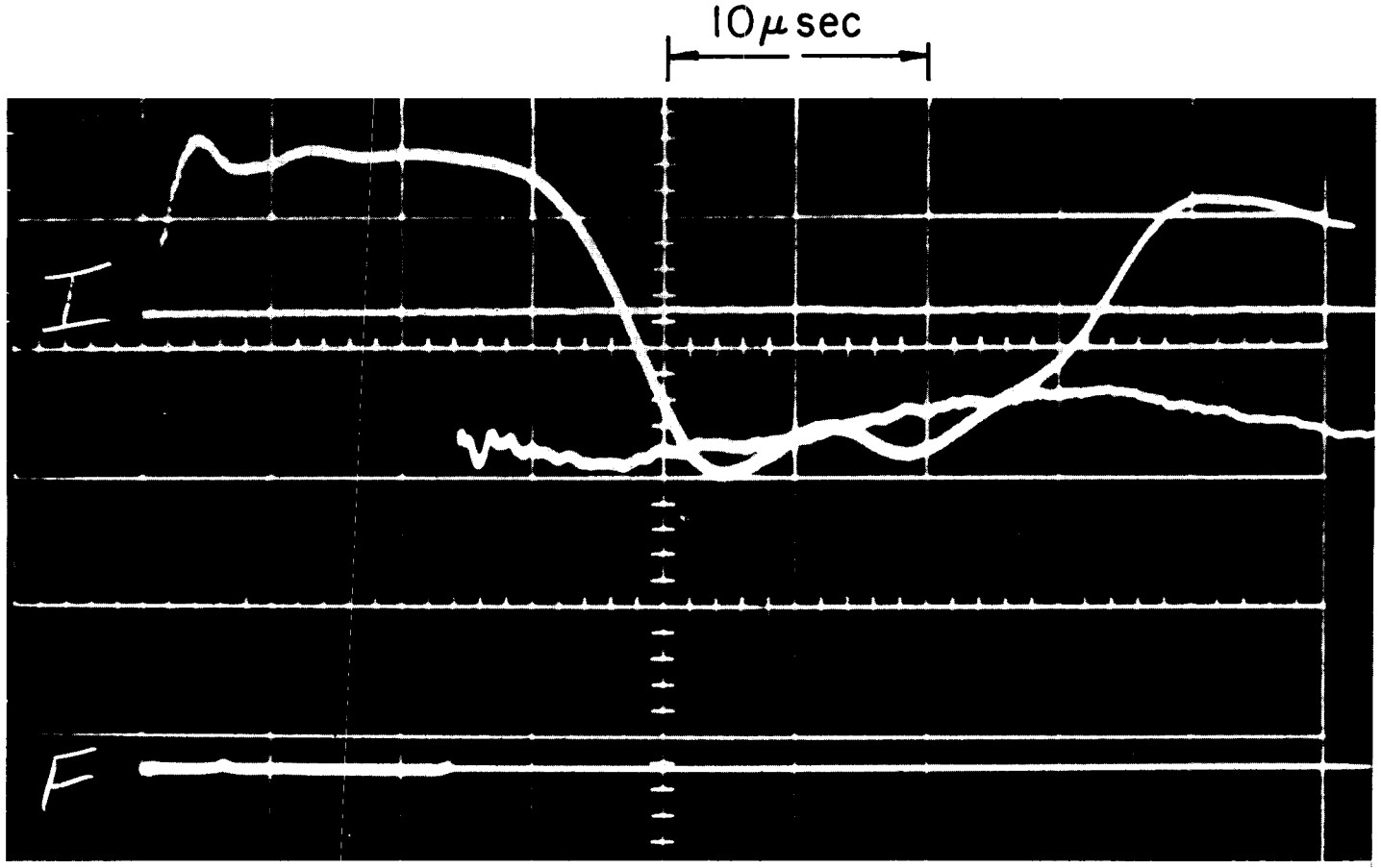

OSCILLOGRAM : DISCHARGE CURRENT I
AND RESPONSE F OF FARADAY CUP

FIGURE 24

VII. VERSATILE, HIGH-PERFORMANCE CAPACITORS (Jahn, Black, Corson)

In the course of design and construction of the first transmission line unit for the tailored-pulse studies, it became evident that no capacitors combining all of the desired features for this type of work were commercially available. Indeed, the two present pulse lines employ capacitors which lack certain desirable characteristics, yet are substantially over-designed in many other respects, and actually are more costly than necessary.

The difficulty seems to be that no capacitor designer and manufacturer has seriously devoted himself to the rather unique requirements for units for pulsed plasma propulsion work. The desired characteristics for such units--low internal inductance, low conductance, small size and weight, convenient and low inductance terminations, "piggy-back" superposibility, and good lifetime in pulsed operation, are by no means fundamentally difficult, and should not require a high price unit, but prior to this effort, no manufacturer geared to this type of work had undertaken the problem.

Roughly one year ago, Mr. Donald Corson, president of Corson Manufacturing Corp., whose standard capacitor units we have employed in several of our discharge devices, expressed interest in this problem and upon his own initiative and resources prepared a few sample units which represented substantial improvements in this type of capacitor. Accordingly, funds were included in the current grant specifically to further this type of study.

The first systematic attack on the subject involved the construction of five low voltage capacitors, all of the rectangular configuration shown in Fig. 25a, but of various combinations of dimensions, A, B, C. After a series of measurements on the observed resonant frequencies of these capacitors, a second set of trial units were constructed and tested in similar fashion. On the basis of these two studies, an optimum assignment of dimensions for our purposes could be made, taking into account not only the inductance/capacitance ratio, but matters of convenient attachment to a line, minimization of terminal inductance, and minimum interference with associated apparatus. Models of this unit were then constructed and tested, and following further minor changes, the prototype, high voltage version is now under construction.

As designed, this unit will have the form shown in Fig. 25b with dimensions of about A = 8", B = 8", and C = 10". It will

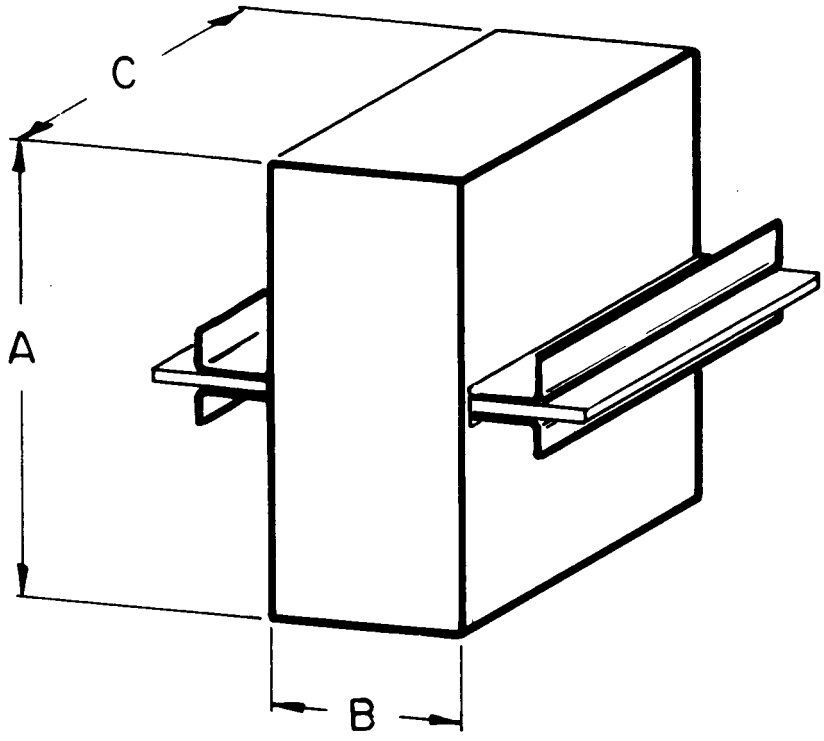

a) LOW VOLTAGE UNIT

b) PROTOTYPE UNIT

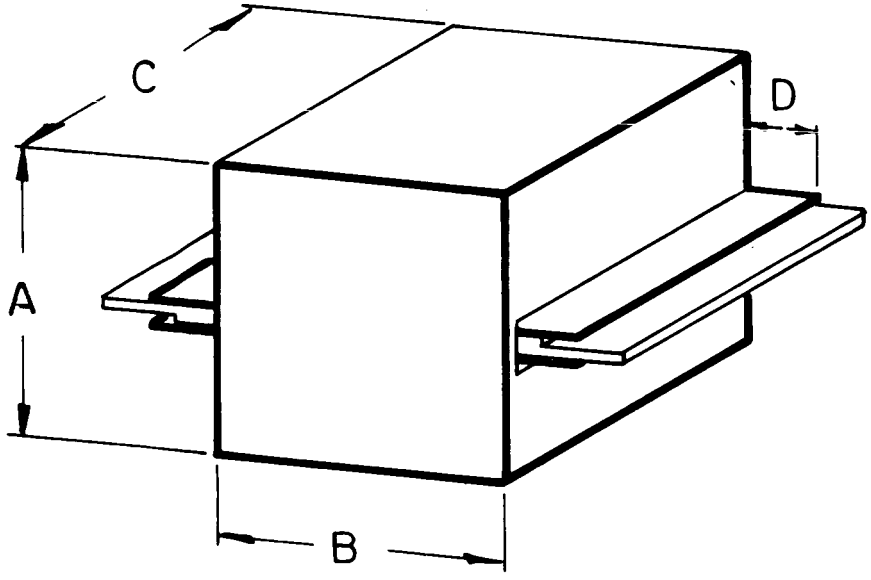

AP25-4095-66

DESIGN OF HIGH PERFORMANCE CAPACITORS

FIGURE 25

have a capacity of about 7 μfd and a resonant frequency above 2 mc. Its double plate terminals will lend themselves to construction of very low impedance lines. Indeed, adjacent capacitors may be attached directly to each other with no separating elements whatever. It is hoped thereby to achieve a pulse-forming line of impedance in the 0.010 ohm range which will essentially match the typical 8" pinch discharge.

VIII. LARGE PLEXIGLAS VACUUM FACILITY
(Jahn, von Jaskowsky, Clark)

The importance of a vacuum vessel which provides minimum interference with the exhaust plume is quite evident, and has been clearly demonstrated by previous experiments in this laboratory and elsewhere. The essential properties involved in such a facility are its dimensions, its material, and its vacuum properties. It must be large enough that the exhaust plume does not propagate to any of its walls during the desired observation times. Its material should not sustain any current conduction along its surface, nor sustain any induced currents or other magnetic interactions which could prejudice the electrical characteristics of the plume. Finally, it should be capable of attaining and sustaining a sufficiently hard vacuum that mean free paths in the ambient gas are larger than the tank dimensions. Thus, we are committed to a dielectric vacuum vessel, several cubic meters in volume, capable of operation in the range of 10^{-5} mm. Hg. (Torr).

Design and construction of such a facility has proven far from trivial. No glass manufacturer was willing to undertake the task at any price. Two bids were received from plastic specialty houses, for heavy-wall Plexiglas construction. Initial concern about the vacuum properties of Plexiglas were allayed by data supplied by the manufacturer, Rohm and Haas Co. (Bristol, Pa.), which indicated a tolerable outgassing level for the preferred material, Plexiglas G. Use of this material provided the added advantages of simple machining, chemical welding, and a transparent final product.

The tank was designed at our laboratory in collaboration with the chosen fabricator, Edcraft Industries, Inc., (Linden, N. J.). It is in the form of a cylinder, 3 feet in diameter, 6 feet long, with a hemispherical fixed end, and a dish-shaped removable end. Ports are provided for the plasma accelerator at the removable end, for the ion probe and other beam diagnostics at the fixed end, and each side has four large access ports for pumping equipment, gauges, other diagnostic instrumentation, and photographic purposes. Fig. 26 shows a design drawing of this vessel.

The main body of the vessel was formed by heating a 1-inch thick plane sheet of the material to about 300° F and allowing it to drape itself over a half-cylinder mandrel, whence it was allowed to cool. Two half-cylinders thus formed were trimmed, and cemented together with a "PS-18" compound containing methyl methacrylate monomer and polymer, a base resin, a catalyst, and a promoter compound. The fixed hemispherical end was vacuum

AP25-4098-66

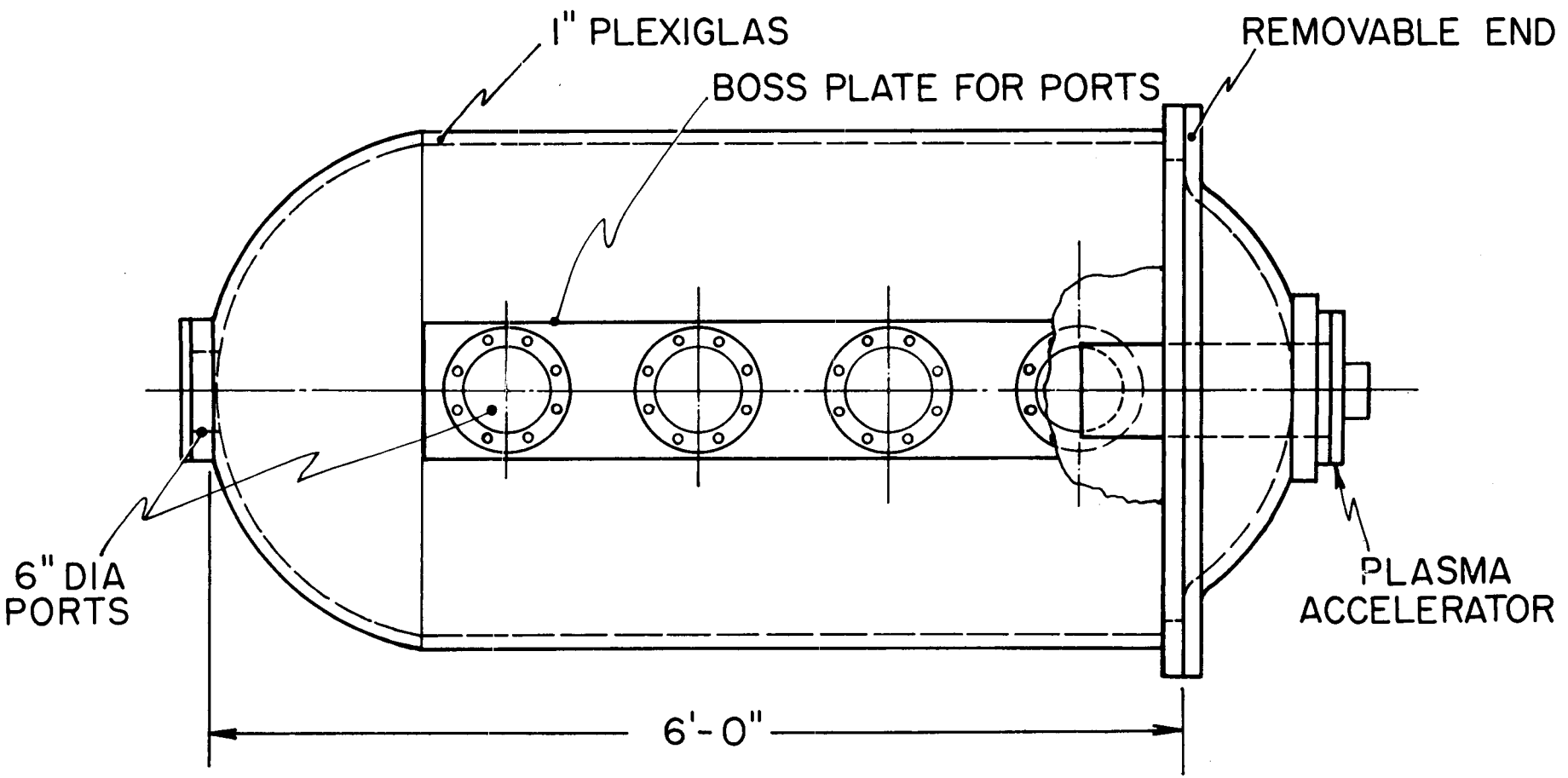

DESIGN DRAWING OF PLEXIGLAS VACUUM TANK

FIGURE 26

formed in a suitable "plug-assist" mold from a similarly pre-heated 1-inch sheet of Plexiglas. After trimming, it was cemented onto the cylindrical member. The removable, dish-shaped end was free-formed in the same way. Two 1-1/2-inch thick strips of Plexiglas were fitted and cemented to the curvature of the cylinder over its entire length to serve as bosses for the four 6-inch ports on the side walls. These ports were provided with interchangeable Plexiglas covers of 1/2-inch plate. Figure 27 shows photographs of the completed product.

The tank is equipped with a CVC 6-inch oil diffusion pump, Type PAS-61, a freon-cooled baffle, a 6-inch gate valve, and a 15 cfm forepump. A few initial leaks in certain "O"-ring grooves were readily eliminated with the aid of a CEC Type 24-120 Helium Leak Detector (sensitivity 1 part He to 10^7 parts air at 0.2 μ), after which the tank pumped down directly to 0.01 μ. This is already an acceptable operating pressure from the mean free path criterion ($\lambda \approx \frac{5 \text{ cm}}{p(\mu)}$ for argon), but can probably be lowered further by lengthy pumping. At present, the pressure rise when the pump valve is closed varies from about 0.7 μ/min. initially to about 0.1 μ/min. after 24 hours.

The composition of the gas in the tank at its present ultimate pressure has been analyzed with a CEC "Diatron" mass spectrometer and found to be 88% water vapor, 11% air, and 1% argon plus assorted hydrocarbons. Thus, it appears that surface adsorption of water vapor, rather than leaks or Plexiglas sublimation will be the essential limitation on the vacuum limits of this device.

Independent data on the behavior of Plexiglas under high vacuum conditions are very sparse, and in poor agreement. As an example, Fig. 28 shows initial outgassing rate variation with total pumping time, data for which have been taken from references II-6 and II-7. The curves have been extended to bring them into the diffusion pump through put range at 0.01 μ which is approximately 20 μ-liter/second. This figure indicates that to bring the tank down to 0.01 μ requires 60 or more pumping hours, depending on the true outgassing rate. However, since the primary outgassed material from Plexiglas is water vapor, subsequent pump-downs do not require the same amount of time as long as the tank has been filled with a dry inert gas in the interim period.

At the present time, the first series of exhaust studies to be performed in this tank have just begun. Results on these and subsequent experiments, as well as further data on the vacuum behavior of the tank will be presented in the next report.

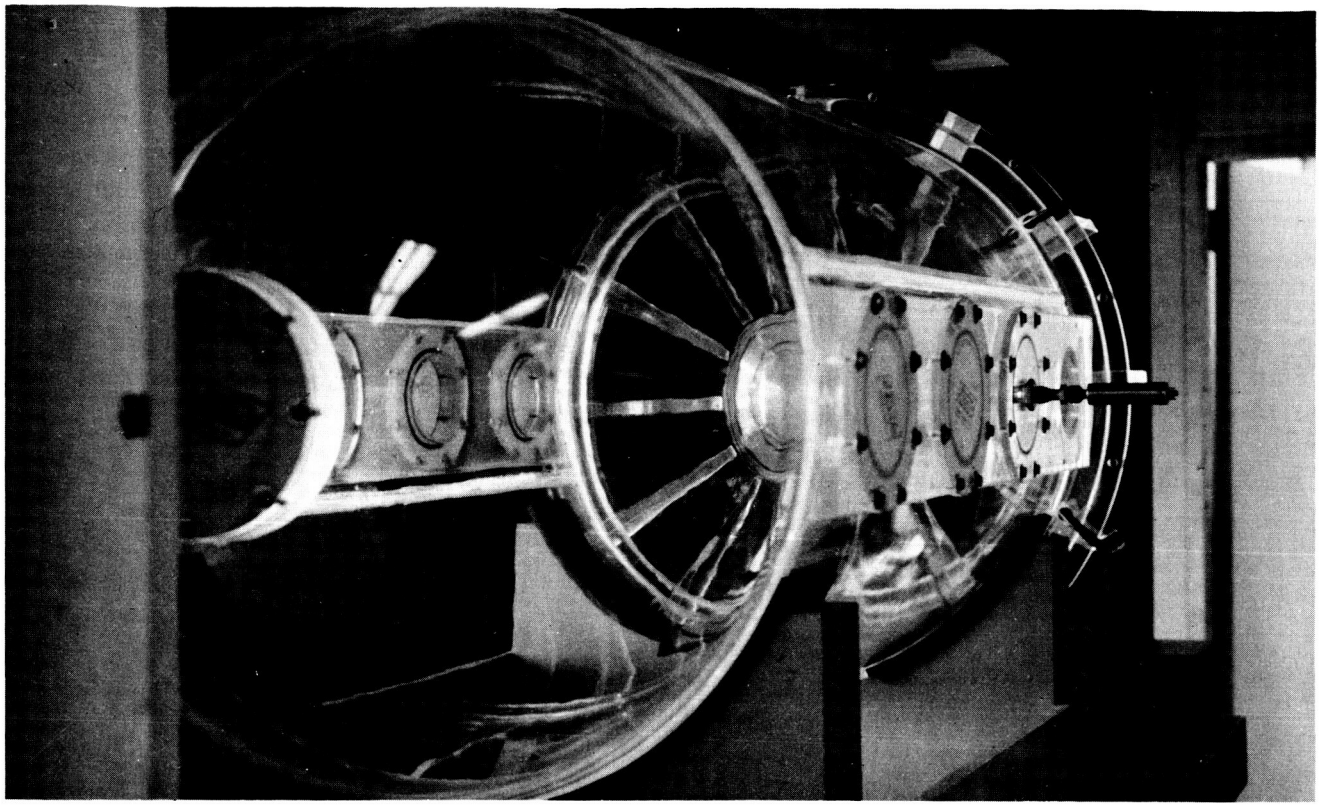

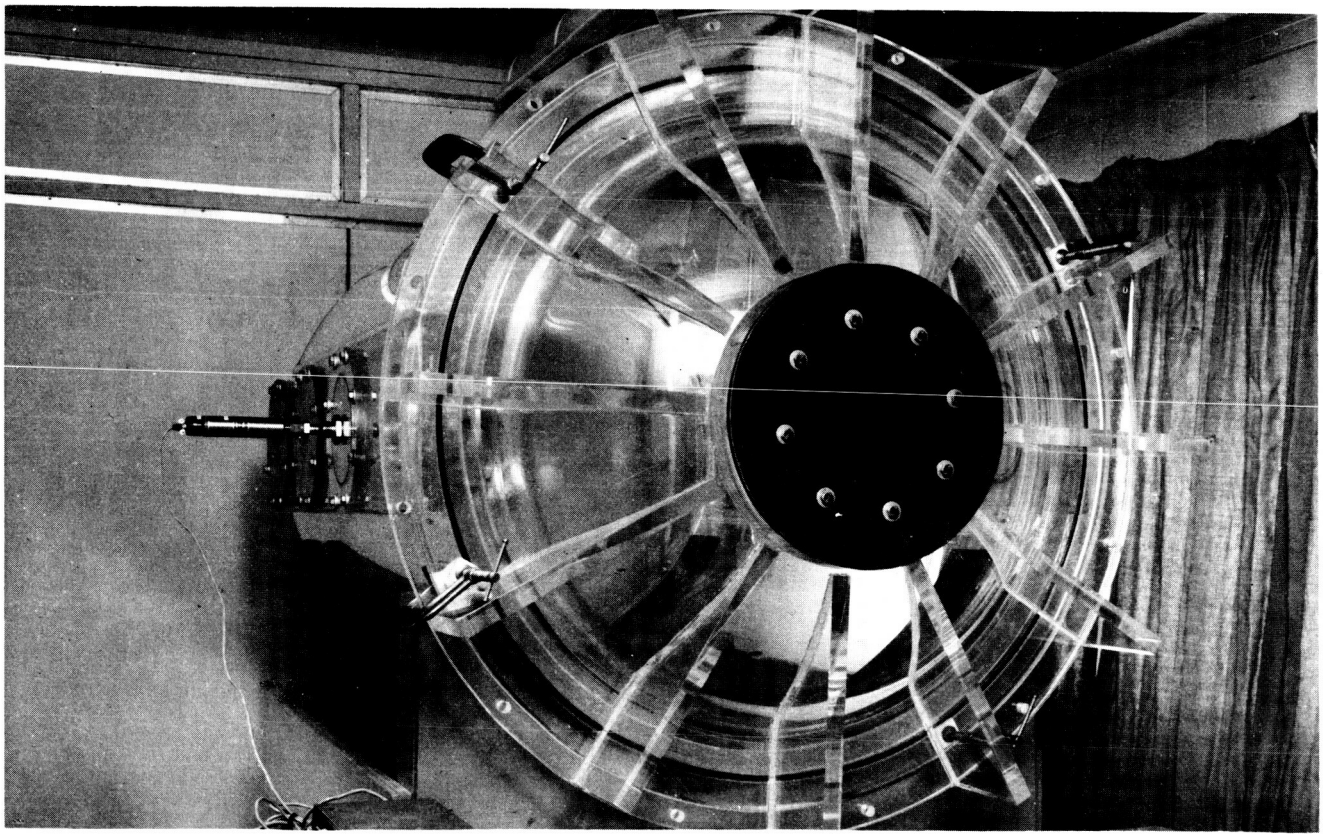

APS5-P47-66

PHOTOGRAPHS OF LARGE PLEXIGLAS VACUUM TANK

FIGURE 27

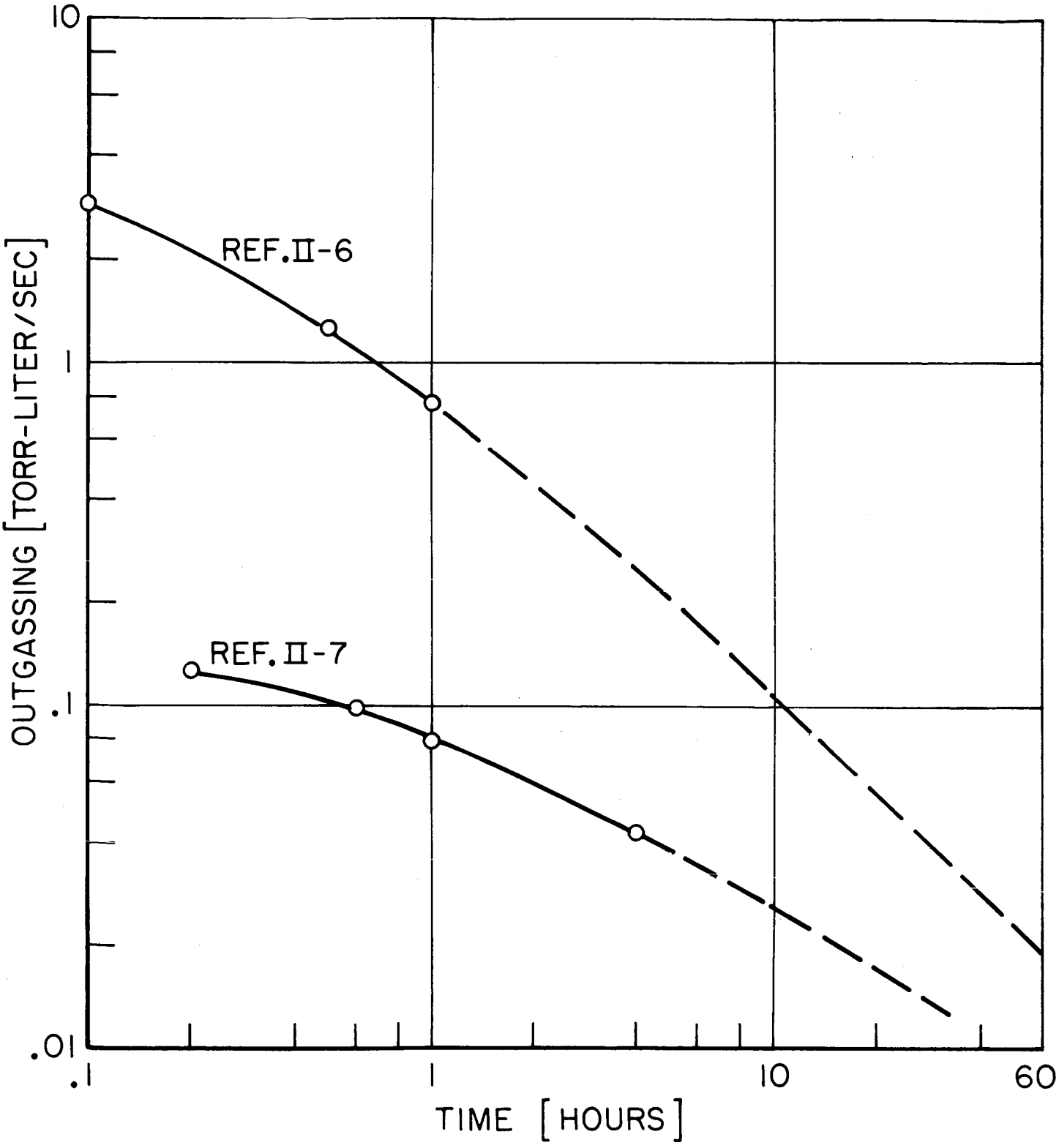

AP25-4097-66

OUTGASSING RATE OF PLEXIGLAS

FIGURE 28

I. Project References

I-1. "Proposed Studies of the Formation and Stability of an Electromagnetic Boundary in a Pinch." Proposal for NASA Research Grant NsG-306-63, 5 March 1962.

I-2. First Semi-Annual Progress Report for the period 1 July 1962 to 31 December 1962, Research Grant NsG-306-63, Aeronautical Engineering Report No. 634, Princeton University, Princeton, New Jersey.

I-3. "The Plasma Pinch as a Gas Accelerator," AIAA Electric Propulsion Conference, 11-13 March 1963, Preprint No. 63013.

I-4. Second Semi-Annual Progress Report for the period 1 January 1963 to 30 June 1963, Research Grant NsG-306-63, Aeronautical Engineering Report No. 634-a, Princeton University, Princeton, New Jersey.

I-5. "Structure of a Large-Radius Pinch Discharge," AIAA Journal 1, 8, 1809-1814 (1963).

I-6. "Gas-Triggered Inverse Pinch Switch," Review of Scientific Instruments 34, 12, 1439-1440 (1963).

I-7. "A Gas-Triggered Inverse Pinch Switch," Technical Note, Aeronautical Engineering Report No. 660, Princeton University, Princeton, New Jersey, August, 1963.

I-8. "Pulsed Electromagnetic Gas Acceleration," Paper No. II, 8, Fourth NASA Intercenter Conference on Plasma Physics in Washington, D. C., 2-4 December 1963.

I-9. "Current Distributions in Large-Radius Pinch Discharges," AIAA Aerospace Sciences Meeting, 20-22 January 1964, AIAA Preprint No. 64-25.

I-10. "Current Distributions in Large-Radius Pinch Discharges," AIAA Bulletin 1, 1, 12 (1964).

I-11. "Current Distributions in Large-Radius Pinch Discharges," AIAA Journal 2, 10, 1749-1753 (1964).

I-12. Third Semi-Annual Progress Report for the period 1 July 1963 to 31 December 1963, Research Grant NsG-306-63, Aeronautical Engineering Report No. 634-b, Princeton University, Princeton, New Jersey.

I-13. "Pulsed Electromagnetic Gas Acceleration," Renewal Proposal for 15 months extension of NASA Research Grant NsG-306-63, Princeton University, Princeton, New Jersey, dated 15 January 1964.

I-14. Fourth Semi-Annual Progress Report for the period 1 January 1964 to 30 June 1964, Research Grant NsG-306-63, Department of Aerospace and Mechanical Sciences Report No. 634c, Princeton University, Princeton, New Jersey.

I-15. "Gas-Triggered Pinch Discharge Switch," Princeton Technical Note No. 101, Department of Aerospace and Mechanical Sciences, Princeton University, Princeton, New Jersey, July 1964.

I-16. "Gas-Triggered Pinch Discharge Switch," The Review of Scientific Instruments 36, 1, 101-102 (1965).

I-17. "Double Probe Studies in an 8" Pinch Discharge," M.S.E. Thesis of J. M. Corr, Department of Aerospace and Mechanical Sciences, Princeton University, Princeton, New Jersey, September 1964.

I-18. "Exhaust of a Pinched Plasma from an Axial Orifice," AIAA Bulletin 1, 10, 570 (1964).

I-19. "Exhaust of a Pinched Plasma from an Axial Orifice," AIAA Second Aerospace Sciences Meeting, New York, New York, 25-27 January 1965, Paper No. 65-92.

I-20. "Ejection of a Pinched Plasma from an Axial Orifice," AIAA J. 3, 10, 1862-1866 (1965).

I-21. Fifth Semi-Annual Progress Report for the period 1 July 1964 to 31 December 1964, Research Grant NsG-306-63, Department of Aerospace and Mechanical Sciences Report No. 634d, Princeton University, Princeton, New Jersey.

I-22. "On the Dynamic Efficiency of Pulsed Plasma Accelerators," AIAA J. 3, 6, 1209-1210 (1965).

I-23. "Linear Pinch Driven by a High-Current Pulse-Forming Network," AIAA Bulletin 2, 6, 309 (1965).

I-24. "Linear Pinch Driven by a High Current Pulse-Forming Network," 2nd AIAA Annual Meeting, San Francisco, California, 26-29 July 1965, Paper No. 65-336.

I-25. "The Design and Development of Rogowski Coil Probes for Measurement of Current Density Distribution in a Plasma Pinch," M.S.E. Thesis of Edward S. Wright, Department of Aerospace and Mechanical Sciences, Princeton University, Princeton, New Jersey, May 1965.

I. Project References-contd.

I-26. "The Design and Development of Rogowski Coil Probes for Measurement of Current Density Distribution in a Plasma Pinch," Department of Aerospace and Mechanical Sciences Report No. 740, Princeton University, Princeton, New Jersey, June 1965.

I-27. "Pulsed Electromagnetic Gas Acceleration," Renewal Proposal for 12 months extension of NASA Research Grant NsG-306-63, Princeton University, Princeton, New Jersey, dated 7 June 1965.

I-28. "Minature Rogowski Coil Probes for Direct Measurement of Current Density Distributions in Transient Plasmas," Rev. Sci. Inst. 36, 12, 1891-1892 (1965).

I-29. Sixth Semi-Annual Progress Report for the period 1 January 1965 to 30 July 1965, Research Grant NsG-306-63, Department of Aerospace and Mechanical Sciences Report No. 634e, Princeton University, Princeton, New Jersey.

I-30. "Cylindrical Shock Model of the Plasma Pinch," M.S.E. Thesis of Glen A. Rowell, Department of Aerospace and Mechanical Sciences, Princeton University, Princeton, New Jersey.

I-31. "Cylindrical Shock Model of the Plasma Pinch," Department of Aerospace and Mechanical Sciences Report No. 742, Princeton University, Princeton, New Jersey.

I-32. "Pulse Forming Networks for Propulsion Research," paper to be presented at the Seventh Symposium on Engineering Aspects of Magnetohydrodynamics, at the Princeton University, Princeton, New Jersey, March 30-April 1, 1966.

II. General References

II-1. R. Lovberg, "Inference of Plasma Parameters from Measurement of $\vec{E}$ and $\vec{B}$ Fields in a Coaxial Accelerator," Phys. of Fluids 7, S57 (1964).

II-2. Fillipov, N. V., "Investigation of Pressure in a Powerful Pulsed Gas Discharge Using a Piezoelectric Measuring Device," Plasma Physics and the Problems of Controlled Thermonuclear Reactions (Pergamon Press, N. Y., 1959), Vol. III, p. 280.

II-3. Vlases, G. C., "Experiments on a Cylindrical Magnetic Shock Tube," J. Fluid Mechanics, V. 16, I, 82 (1963).

II-4. J. A. Stratton, "Electromagnetic Theory," (McGraw Hill Book Co., N. Y., 1941).

II-5. Ashby, D. E. T. F., Gooding, T. J., Hayworth, B. R. and Larson, A. V., "Exhaust Measurements on the Plasma from a Pulsed Coaxial Gun," AIAA J. 3, 6, 1140-1142 (1965).

II-6. Santeler, D. J., Outgassing Characteristics of Various Materials, American Vacuum Society, 5th Vacuum Symposium, 1958, (Pergamon Press, N. Y., 1959), pp. 1-8.

II-7. Schittko, F. J., Measurement of Gas Emission from Solid Surfaces, Vacuum, V. 13, pp. 525-537, Dec. 1963.